Faunal and stratigraphic analysis of the basal Cretaceous-Paleogene (K-Pg) boundary event deposits, Brazos River, Texas, USA

Kayla M. Irizarry[1], James D. Witts[2], Matthew P. Garb[3], Anastasia Rashkova[4], Neil H. Landman[4], Mark E. Patzkowsky[1]

[1] Department of Geosciences, Pennsylvania State University, University Park, PA 16802, USA

[2]Bristol Palaeobiology Research Group, School of Earth Sciences, University of Bristol, Bristol, BS8 1RJ, UK

[3]Department of Earth and Environmental Sciences, Brooklyn College, Brooklyn, New York 11210, USA

[4]Department of Invertebrate Paleontology, American Museum of Natural History, New York, New York 10024, USA

Abstract

A bolide impact ~66 million years ago near Chicxulub, Yucatan Peninsula, Mexico triggered environmental perturbations on a global scale, leading to mass extinction at the Cretaceous-Paleogene (K-Pg) boundary. Outcrops on the U.S Gulf Coastal Plain that contain the K-Pg boundary provide a detailed record of environments across this critical transition, but questions remain about the nature and timing of depositional processes that affected the region at the time of impact and mass extinction. We present a new study of coarse-grained K-Pg 'event deposits' located at the contact between the fossiliferous Cretaceous Corsicana Formation and the Danian Kincaid Formation, and which outcrop in tributaries along the Brazos River, Falls County, Texas. A generalized succession can be recognized in these deposits. We sampled the basal-most unconsolidated units, Unit I and Unit II, and the Corsicana Formation for macrofaunal and sedimentological data. Unit I is interpreted as a debrite, deposited by a medium – high strength cohesive debris flow initiated by ground shaking and intense seismic activity after the Chicxulub impact. Macrofossil analysis shows a mostly locally derived assemblage. Grain size analysis of non-carbonate portions of the matrix indicates an identical mean grain size to that of the underlying Corsicana Formation. The chaotic fabric, boulder sized clasts, and muddy matrix support the

interpretation of deposition via cohesive debris flow. Unit II is also interpreted as a debrite, deposited by a low-medium strength cohesive debris flow. We propose that this unit was initiated by wave energy from a tsunami or local shelf collapse immediately following impact. Macrofossil analysis of Unit II shows an increase in fauna with a predatory/carnivorous lifestyle, which are interpreted as allochthonous elements derived from shoreward environments and transported across the shelf. The high mud content of the matrix and abrupt pinching out on topographic highs support the interpretation of deposition via a cohesive debris flow for Unit II. Our results indicate that sediment flows were a major driver of mass sediment transport in proximal locations directly following the Chicxulub impact.

Keywords

Cretaceous, Paleogene, Mass Extinction, K-Pg, Debris flow, Sediment flow

1. Introduction

1.1. Background

The Cretaceous–Paleogene (K-Pg) mass extinction resulted in a profound loss of biodiversity that altered the course of evolutionary history. The K-Pg is the most recent of "the big five" mass extinctions of the Phanerozoic, responsible for the loss of 40% of genera and more than 70% of species worldwide (Raup and Sepkoski, 1982; Bambach, 2006). The Chicxulub bolide impact, ~66 my, is posited as the main driver of the K-Pg extinction event (Alvarez et al., 1980; Schulte et al., 2010; Hull et al., 2020; During et al., 2022). Possible global effects of the impact include a period of global darkness due to injection of sulfur aerosols, soot, and ejecta into the atmosphere. This led to a sharp reduction in photosynthetic activity and food chain collapse (Sheehan and Hansen, 1986), rapid and sustained cooling (Brugger et al., 2017; Vellekoop et al., 2016; Lyons et al., 2020; Junium et al., 2022), and ocean acidification (Henehan et al., 2019).

Locally, the impact may have caused tsunamis, storm surges, deposition of impact related ejecta, and mass movement of sediment, (Yancey and Liu, 2013; DePalma et al., 2019; Gulick et al., 2019; Kinsland et al., 2021). In the deep-water settings of the Gulf of Mexico the K-Pg boundary coincides with

seismically induced debris flow and landslide deposits, which collectively comprise the largest mass flow deposits on Earth (Denne et al., 2013; Sanford et al., 2016; Poag, 2017). In shallow water settings, a variety of sections in Mexico and the Gulf Coastal Plain, USA, document local conditions immediately preceding and following impact (Bourgeois et al., 1988; Smit et al., 1996; Yancey, 1996; Bohor, 1996; Schulte et al., 2012; Yancey and Liu, 2013; Sanford et al., 2016; Witts et al., 2018; Hart et al., 2019). These sections contain complex stratigraphic records. Untangling the depositional processes recorded by these sediments contributes to our understanding of the scale and duration of events directly caused by the Chicxulub impact event. This allows for more accurate modeling of proximal biotic and environmental effects in shelf settings, and a clearer understanding of the drivers and potential 'kill mechanisms' of the K-Pg mass extinction.

Sites exposed along the Brazos River in Falls County, Texas, represent proximal K-Pg boundary sections, located around 1500 km from Chicxulub (Schulte et al., 2010) and contain an expanded, apparently continuous record of deposition from the Upper Cretaceous (Corsicana Formation) and Lower Paleocene (Kincaid Formation). Outcrops in this area also contain a complex of coarse-grained 'event deposits' coincident with the formational contact (Bourgeois et al., 1988; Hansen et al., 1987; Hansen et al., 1993a). These deposits exhibit considerable lateral variability in thickness and internal stratigraphy within a small (5 km^2) area south of the Texas Rt. 413 bridge (Fig. 1) (e.g., Adatte et al., 2011; Hart et al., 2012; Yancey and Liu, 2013; Hart et al., 2019; Witts et al., 2021), and have been divided into as many as seven distinct units (Hansen et al., 1987; Hansen et al., 1993a; Smit et al., 1996; Schulte et al., 2006) some of which may repeat or be absent in any given outcrop.

Despite this complexity a generalized succession of sediment types is recognizable in these deposits; **1)** a basal mudstone-clast-bearing unit with a bioclast rich muddy matrix (unit B of Hansen et al. (1987); 'Basal Conglomerate Bed'/BCB of Yancey (1996) and Yancey and Liu (2013); referred to here as **Unit I**), overlain by **2)** an ejecta-spherule-rich coarse sandstone (unit C of Hansen et al. (1987); 'Spherulitic Conglomerate Bed'/'SCB' of Yancey (1996) and Yancey and Liu (2013); referred to here as **Unit II**), followed by **3)** cross-bedded sandstones interbedded with siltstones (often referred to as the

78 ‘sandstone complex’; units D and E of Hansen et al. (1987); ‘Hummocky-Sandstone unit/‘HCS’ and
79 ‘Granular Sandstone Bed’/’GSB’ of Yancey (1996) and Yancey and Liu (2013)), capped by **4)** an
80 upward-fining layer of siltstone and mudstone which contains one or multiple weak iridium anomalies
81 (units E-G, H of Hansen et al. (1987)’ ‘Calcareous Clayey Horizon’/‘CCH’) (Yancey, 1996; Yancey and
82 Liu, 2013) (Fig. 2). The mass extinction of Cretaceous micro- and macrobiota is coincident with these
83 units (Hansen et al., 1987; Hansen et al., 1993a; Yancey, 1996; Yancey and Liu, 2013; Smit et al., 1996;
84 Bralower et al., 2010; Hart et al, 2019; Witts et al., 2021). The sequence is overlain by the Littig Member
85 of the Kincaid Formation which records a return to pre-impact conditions.
86 The focus of this study is the basal mudstone clast–bearing unit (Unit I) and the overlying ejecta-
87 spherule-rich coarse sandstone unit (Unit II) (Fig. 2, Fig. 3, Fig. 4). These fossiliferous semi-consolidated
88 units have not previously been the subject of focused study, partly due to the stratigraphic complexity
89 outlined in the previous paragraph, and because they do not occur consistently in all exposures of the K-
90 Pg deposit across the Brazos outcrop belt. The locality chosen for this study, Darting Minnow Creek,
91 preserves expanded outcrops of Unit I and Unit II. Previous studies focused primarily on deposits along
92 the main Brazos River bed where these units do not appear or are significantly less expanded in outcrop
93 (Hansen et al., 1987; Hansen et al., 1993a; Yancey and Liu, 2013; Hart et. al., 2019). We provide new
94 and detailed descriptions of the macrofaunal assemblages, stratigraphic architecture, sedimentary
95 structures, and sedimentology (e.g., fabric, packing, grain size). Pairing new observations with existing
96 datasets allows us to constrain depositional processes, energy, and timing in more detail than was
97 previously possible.
98 Previous interpretations of these units have proved contentious, as has the placement of the K-Pg
99 boundary within the sequence (e.g., Schulte et al., 2006; Keller et al., 2007; Hart et al., 2012). Prior
100 research has interpreted Unit I as a debris flow deposit (Yancey, 1996; Schulte et al., 2006) while Unit II
101 has been interpreted as a tsunami deposit (Bourgeois et al., 1988; Smit et al., 1996) or a winnowed lag
102 created by large storms post-impact (Yancey and Liu, 2013). Alternatively, some authors do not consider
103 any part of the K-Pg boundary complex at Brazos to be impact related; instead interpreting these

sediments as large storm deposits (in this case unrelated to impact), or channel sands deposited during a sea level lowstand prior to the K-Pg boundary and mass extinction (Keller et. al. 2007; Adatte et al., 2011).

Recent work has sought to resolve these issues and develop a litho- and biostratigraphic framework that can be accurately correlated to the international timescale (e.g., Hart et al., 2012; 2019; Yancey and Liu, 2013; Leighton et al., 2017; Witts et al., 2021). In these studies, the K-Pg boundary is recognized according to the formal ICS definition based on the sequence at the GSSP in El Kef, Tunisia. This states that the boundary is best tied to the "moment of the meteorite impact, which implies that all the sediments generated by the impact belong to the Danian" (Molina et al., 2006). While there is a degree of circularity in this argument (see Hart et al., 2019 for discussion), it has important implications for interpreting these successions as outlined below.

1.2. Geological setting

The Corsicana Formation and overlying Kincaid Formation exposed along the Brazos River represent a shallow marine, mid-shelf depositional environment at the time of the Chicxulub impact event. Water depth interpretations using foraminiferal assemblages suggest both the Corsicana and the Kincaid formations were deposited below storm wave base (ca. 75-100m; Hart et al., 2012; Yancey and Liu 2013; Woelders and Speijer, 2015); macrofossils suggest similar or slightly shallower depths (Witts et al., 2021). Mid to outer shelf conditions generally characterize the latest Cretaceous and earliest Paleogene in this area, which was located around 100 km to the east of the Cretaceous shoreline at the central Texas uplift, with the shelf-slope margin located around 150 km to the south (Galloway, 2000). Low energy fine-grained siliclastic sedimentation resulted in the deposition of shales and siltstones, with occasional sandstone layers (Yancey, 1996; Hart et al., 2012). The contact between the Corsicana and Kincaid formations in this part of Texas generally marks the paleontologically-defined K-Pg boundary (Hart et al., 2012; Yancey and Liu, 2013; Hart et al., 2019). Tectonic deformation in this region is minimal, with minor folding and faulting with a shallow regional dip of 2° to the south (Yancey, 1996; Yancey and Liu, 2013).

2. Methods

2.1. Stratigraphy and sedimentology

Stratigraphic data were collected from outcrops exposed along the Brazos River (the 'Riverbank South' (RBS) section of Hart et al. (2012) and Leighton et al. (2017) (AMNH locality 3968)) and its tributaries, Darting Minnow Creek (DMC) (AMNH locality 3620) and Cottonmouth Creek (CMC) (AMNH locality 3621). The primary focus was the waterfall section at DMC which preserves an expanded ~2 m-thick exposure of the K-Pg boundary complex (Fig. 5). This section appears to have been deposited in a large channel-like feature cut into the Cretaceous-Paleogene sea floor (Figure. 3) (Adatte, 2011; Yancey and Liu, 2013).

An 80 cm-long push core of units I and II was taken at this locality using plastic containers, and a cordless Dremel power tool (Sup Fig. 1). The containers were hammered into place, and the Dremel was used to cut away sediment adjacent to the core for easy and clean removal. Grain size analysis was performed on the insoluble fraction of sediment from the uppermost Corsicana Formation and through units I and II. Samples were taken every 10 cm through the 80 cm thick section. Sediment was treated with 50% hydrochloric acid (HCL) to remove calcium carbonate and 30% hydrogen peroxide (H_2O_2) to remove organic matter. Sediment was then suspended in a 0.5% sodium hexametaphosphate solution. A Malvern Mastersizer 3000 was used to obtain the grain size through laser diffraction. This measures only the fine grain size fraction of sediment (10nm – 3500μ). Note that HCL treatment removes the dominantly carbonate bioclasts from the analyses.

2.2. Faunal Analysis

Bulk samples were collected from the Corsicana Formation and the event deposit (Unit I and Unit II) at the DMC waterfall section (DCM-W). The base of Unit I was used as a datum (Figure. 5). Corsicana Formation samples were taken at 1.25 m (A) and 0.5 m (B) below the datum, weighing 104 kg and 257 kg, respectively. Samples from the event deposit were taken at 20 cm (Unit I) and 40 cm (Unit II) above the datum, weighing 45 kg and 41 kg respectively. Bulk sampling procedure incorporated sediments 10 cm above and below the given sampling interval. Extraction of macrofossils was performed in the field

for the Corsicana Formation and in the laboratory for units I and II. Sediment samples were broken down to <3 cm pieces in both cases. Fossils were extracted and stabilized using Jade 403 adhesive in the lab. Samples extracted in the field were brought back to the lab and stabilized with adhesive when necessary.

Fossils were identified to genera or species level where possible using the published literature (Stephenson, 1955; Sohl, 1960; Hansen et. al. 1987; Hansen et. al., 1993b; Akers and Akers, 2002a, Akers and Akers, 2002b). Only the benthic invertebrate macrofauna (>5mm) were identified in this study. Taxon counts from additional targeted collections of cephalopods from the Corsicana Formation were not included in quantitative analysis and can be found in Witts et al. (2021).

Tiering, mobility, and feeding ecology for each species were determined using the published literature (e.g., Sessa et al., 2012; Aberhan and Kiessling, 2015) and the Paleobiology Database (PBDB). Mode of life analysis was conducted using specimen abundance and species richness counts separately, with raw values transformed to percentages to facilitate comparison between units. Abundance and richness metrics produced nearly identical results, therefore only abundance metrics are presented and discussed.

2.3. Multivariate Statistical Analysis

Cluster analysis of taxa was performed in R v.3.3.3 (R Core Team, 2017), using the packages vegan (Oksanen et. al., 2019) and Cluster v.2.0.7 (Maechler et al., 2018). Analyses were run only on benthic mollusks, in accordance with similar studies from the region (Sessa et al., 2012; Aberhan and Kiessling, 2015). Cluster analyses were carried out using the Bray-Curtis distance measure and Ward's linkage method, on samples from four horizons, two from the Corsicana Formation and one each from units I and II. Prior to analyses the data were transformed by dividing each taxon count by the taxon maximum across all samples to accentuate rarer taxa and prevent abundant taxa from dominating the results (McCune et al., 2002).

3. **Results**

3.1. Stratigraphy

The Corsicana Formation is laterally continuous over the entire study area. An approximately 1.5-meter-thick section is exposed at DMC (AMNH loc. 3620). The lithology varies from laminated shale 1.5 meters below the K-Pg boundary, to more massive mudstone directly beneath the boundary. The contact between the uppermost Corsicana Formation and the K-Pg boundary complex is sharp at the waterfall section in DMC-W (Fig. 2), with an abrupt lithological change from massive mudstone to clast-rich, unconsolidated mud (Unit I). Elsewhere across the ~5 km Brazos outcrop belt, this surface exhibits irregular relief, suggesting either topographic relief on the sea floor onto which the boundary complex was deposited, and/or significant scouring which occurred at the time of the K-Pg boundary (Fig. 3) (e.g., Yancey, 1996; Hart et al., 2012; Yancey and Liu, 2013).

Unit I varies laterally in thickness: it is up to 35 cm thick at DMC-W (AMNH loc. 3620) and 40 cm thick at the waterfall outcrop in CMC (AMNH loc. 3621). However, within the same ~5 m-wide outcrop at DMC-W the unit pinches out completely, such that Unit II directly overlies the Corsicana Formation. Similarly, at CMC (AMNH loc. 3621) ~100 m downstream of the expanded waterfall section Unit I pinches out, with Unit II again resting on top of disturbed Corsicana Formation shales. Unit I is entirely absent at Riverbank South (RBS) (AMNH loc. 3968). There are two observed instances, both in DMC, of soft sediment deformation between Unit I and the underlying Corsicana Formation, with this unit injected (injections are 3 – 7 cm in length) into underlying disturbed shales. Disturbed uppermost Corsicana shales lack the obvious bedding common throughout the rest of the formation and have a less blocky appearance in outcrop (Fig. 4; Sup Fig.1). The contact between units I and II is transitional, shown in the push-core at 25cm – 35cm (Sup. Fig. 1). This ‘transition zone’ has a higher silt content relative to the rest of Unit II and contains a concentration of ovoid micritic clasts and concretions which are allochthonous in origin.

Unit II also varies laterally in thickness. It is up to ~40cm thick at DMC-W and in some outcrops along CMC. However, elsewhere in CMC it pinches out entirely in as little as 2 m laterally (Fig. 4). In other outcrops, such as at AMNH loc. 3968, this unit is no more than 5 mm thick. In the outcrops along the lower part of CMC where Unit I is not present, there are centimeter-scale injections of Unit II into

disturbed Corsicana Formation shales (Fig. 4). Around 100 m downstream from the waterfall at DMC, both units I and II are essentially absent, and a thin (~15 cm-thick) silty sandstone with shell hash, phosphatic grains, and impact spherules, overlain by glauconitic argillaceous-silty chalk lies between the Corsicana Formation and basal mudstones of the Kincaid Formation (locality DMC-E in Henehan et al. (2019), Witts et al. (2021) and Junium et al. (2022)).

3.2. Sedimentology and paleontology

The Corsicana Formation is composed of brown/grey-colored mudstones and shales. Grain size analysis indicated that this unit is fine silt - clay dominated (Fig. 6). The uppermost Corsicana Formation is abundantly fossiliferous containing bivalves, gastropods, and cephalopods, as well as a diverse microfossil fauna (Jiang and Gartner, 1986; Hansen et al., 1987; Abramovich et al., 2011; Witts et al., 2021). Benthic foraminifera both whole and fragmentary (belonging to the genus *Lenticulina*) are abundant and because of their large size are visible to the naked eye (Plummer, 1926; Hart et al., 2012; Leighton et al., 2017). Preservation of original aragonitic and calcitic shell material in mollusks is common. Bivalves are typically preserved as single intact valves (75.00%), and less frequently as fragments ($\leq$ 1/2 single valve, 25.00%). No articulated bivalves were observed in this unit (Sup. Fig. 2) during systematic collecting of benthic molluscs for this study, but some were found during targeted collecting for cephalopods (Witts et al., 2021). Fossils are sometimes preserved in concentrated pyritized pods of fragmented bioclasts, which may represent burrow in-fills on the seafloor. Bioclasts are almost always orientated parallel to the bedding plane.

Unit I is a fossiliferous, mud-clast conglomerate with a very fine to medium silt and clay matrix. The matrix of this deposit shows poor inverse grading (Fig. 6). However, lack of size sorting of abundant mud clasts in this deposit defines it as non-graded overall. The fabric is matrix supported and tightly packed. Bioclasts show no preferred orientation. Large, grey, laminated shale rip-up clasts from the underlying Corsicana Formation are present throughout Unit I. These rip-up clasts are often coated with the muddy, bioclast rich matrix in which they are entrained with unfossiliferous interiors, resembling ‘armored mud balls’ (Bell, 1940). This unit contains a small number of impact spherules; 13kg of this unit

was carefully examined and only one possible spherule was found. However, this unit does appear to contain other impact ejecta in the form of carbonate lapilli (Yancey and Guillemette, 2008). Original molluscan shell material is often preserved although when released from the matrix, it easily crumbles. Bivalves within this unit are preserved as both external and internal molds. Whole single valves are the most frequently observed form of molluscan preservation (70.18% of specimens), shell fragments (≤ 1/2 single valve) are also prevalent (24.91%). Articulated bivalves are present but not common (4.91%) (Sup. Fig. 2).

Unit II is an unconsolidated clay, bioclast-rich, silty sandstone. Grain size analysis shows that the basal portion of this unit is unimodally distributed, mean grain size is medium silt (Fig. 6). Up-section the grain size becomes bimodally distributed, with an increase in very fine - fine sand, and very coarse silt fractions (Fig. 6). There is a decrease in the fine silt fraction, and a modest increase in the clay fraction which is most apparent in the uppermost sample (70cm) (Fig. 6). This unit is highly variable with respect to both sedimentary constituents and fauna. The bulk of bioclasts are in the "transition zone" at the contact with Unit I, bioclasts are sparse in the middle of the unit and show a moderate increase in abundance towards the upper portion (Sup. Fig. 1). This unit contains an appreciable amount of impact ejecta, primarily spherules but also carbonate lapilli. The largest spherule found was ~2.5 mm in diameter. There is some apparent stratigraphic variation in the concentration of impact ejecta; qualitative evaluations of the push-core suggest that the spherules are not abundant until 60 cm above the base. Micritic cement occurs in lenses or sheets throughout this unit. The fabric is weakly-laminated, matrix supported, and tightly packed. Mollusk shells exhibit a preferred orientation along the long axis. There is no evidence of bioturbation. Original shell material is present but not common. Whole single valves are the most frequently observed form of molluscan preservation (60.65% of specimens), shell fragments (≤ 1/2 single valve) are also prevalent (31.61%). There is an increase in articulated specimens (7.75%) compared to the Corsicana Formation (0.00%) and Unit I (4.91%) (Sup. Fig. 2).

3.3. Macrofauna

Species richness in the Corsicana Formation is high, with 27 species recognized in our quantitative collections (Fig. 7). The dominant species in the Corsicana Formation is the bivalve *Breviarca* (*Striarca) webbervillensis* Stephenson, 1941, which constitutes ~38.9% of the total fauna. The genus *Nuculana* constitutes ~27% of the fauna and is the second most abundant non-cephalopod mollusk. Ammonites belonging to the genera *Discoscaphites* and *Eubaculites* and ostreid bivalves are also abundant in the Corsicana Formation (Hansen et al., 1993b; Witts et. al., 2021) but were not included in the quantitative analysis.

The dominant feeding strategy of the benthic molluscan fauna in the Corsicana Formation is suspension feeding (~64%). The dominant tiering positions are shallow infaunal (~47%) and deep infaunal (~36%). The dominant mobility categories are non-motile, attached with a byssus (~37%), regularly moving (~38%), and facultative, unattached (~25%) (Fig. 8).

A total of 22 species occurs in Unit I (Fig. 7). The dominant taxon in this unit is the bivalve *Vetericardiella webbervillensis* Stephenson, 1941, which constitutes ~53% of the total fauna. The dominant feeding strategy of the benthic molluscan fauna in Unit I is suspension feeding (~74%). The dominant tiering position is shallow infaunal (~82%). The dominant mobility category is facultative, unattached (~61%) (Fig. 8).

A total of 24 species occurs in Unit II (Fig. 7). The most dominant taxon in this unit is *Cymbophora cancellosa* Stephenson, 1941, which constitutes ~26% of the fauna. The dominant feeding strategy in Unit II is suspension feeding (61%). The dominant tiering position is shallow infaunal (~59%). The dominant mobility categories are facultative, unattached (~42%), and regularly moving (~35%) (Fig. 8).

Dominant faunal components show a similar ecological pattern between the Corsicana Formation, Unit I, and Unit II. Conversely, each unit contains distinct but less abundant faunal elements (Fig. 8). In Unit II, there is an increase of fauna with a non-motile, attached, cemented lifestyle. In both units I and II, two feeding strategies are present, which do not appear in the underlying Corsicana Formation: herbivore/grazing and surface deposit feeding. In Unit II, there is an increase in abundance of fauna with

a carnivore/predatory feeding strategy. Overall, both Unit I and Unit II show a greater diversity in the ecological habit of their faunal assemblages than the Corsicana Formation despite both having a lower overall species richness (Fig. 8).

3.4. Cluster Analysis

Cluster analysis of species produced five clusters (Fig. 9). Cluster D contains taxa that are abundant in all three units, with one exception, *Nuculana coloradoensis*, which does not occur in Unit I. Cluster E contains taxa most common in the Corsicana Formation, with three exceptions: Turitella (*Haustator) bilira* Stephenson, 1941, *Nuculana Corsicana* Stephenson, 1941 (both of which occur in all units) and *Nuculana houstoni* Stephenson, 1941, which occurs in all units except Unit II. Cluster C contains taxa that occur exclusively in Unit I, with one exception, *Nuculana corbetensi* Stephenson, 1941*s*, which also occurs in the Corsicana Formation. Cluster B contains taxa that occur exclusively in the Corsicana Formation at -1.25 m with one exception, *Cymbophora scabellum* Stephenson, 1941, which also occurs in Unit I. Cluster A contains taxa that occur exclusively in Unit II, with three exceptions: *Nemodon eufalensis Gabb, 1860*, *Synclonema simplicus* Stephenson, 1941, and *Pecten* sp.1, all of which also occur in Unit I.

In summary, there are core taxa that are present and relatively abundant in all three units, for example, *Breviarca* (*Striarca) webbervillensis*. Then there are sets of taxa which are unique to each unit, with overlap most commonly between units that are stratigraphically adjacent to one another.

4. Discussion

The detailed stratigraphic, sedimentological, and faunal data show that each of these three units exhibit distinct features and faunal content, suggesting they also record three different depositional processes. We suggest that depositional processes responsible for Unit I and Unit II can be tied to the local effects of the Chicxulub impact event.

4.1. Placement of the Cretaceous-Paleogene boundary

As mentioned previously, there has been considerable disagreement about the placement of the K-Pg boundary at Brazos (see Schulte et al., 2006; Keller et al., 2007; Bralower et al., 2010; Hart et al.,

2012). This is partly a result of the complex local stratigraphy, and partly due to global changes in thickness of impact deposits relative to the Chicxulub crater. The GSSP section for the base of the Danian in El Kef, Tunisia is an excellent example of a site distal (>5000 km) to the crater, where physical and geochemical evidence for the impact such as ejecta and an iridium anomaly coincide precisely with mass extinction of Cretaceous calcareous micro- and nannofossils in a thin clay layer (see Molina et al., 2006; Schulte et al., 2010). In proximal sections around the Gulf of Mexico these phenomena are often separated or contained within clastic deposits with evidence for high-energy deposition and sedimentary disturbances (Bralower et al., 2010; Schulte et al., 2010; Witts et al., 2018).

We place the K-Pg boundary at the base of Unit I (equivalent to the base of unit B of Hansen et al. (1987); 'BCB' of Yancey (1996) and Yancey and Liu (2013)) (Figs 2, 3). We argue that this is consistent not only with our sedimentological data but with the formal definition ratified by the ICS (Molina et al., 2006), with the presence of impact ejecta in Unit I and Unit II linking these units genetically to the Chicxulub impact. We confirm previous reports that abundant carbonate accretionary lapilli are present within both units I and II (Yancey and Guillemette, 2008). Lapilli found at Brazos River localities have been tied to the Chicxulub impact based on their elevated sulfur content (0.3 to 0.8 wt % SO_3), clumped isotope values which suggest formation at elevated temperatures (>150° C) consistent with modelled temperatures within the impact plume, and their aggregate texture suggesting they formed via accretion from back-reaction of decomposition products following vaporization of carbonate target rock (Yancey and Guillemette, 2008; Burrtt et al., 2022). Similar carbonate lapilli have been identified at other proximal and intermediate K-Pg boundary sites (Pope et al., 2005; Salge et al., 2021). Other ejecta in the form of pseudomorphs of originally glassy impact spherules are also present in Unit I (rare) and common in Unit II (Sup. Fig. 3), exhibiting identical morphologies to other localities around the Gulf of Mexico (Smit et al., 1996; Kring and Petruny, 2008; Witts et al., 2018). Wave-length dispersive electron microprobe analysis of the Brazos spherules show that they are composed mainly of smectite and chlorite minerals and are therefore also chemically similar to altered impact spherules found at proximal and

intermediate K-Pg sites (Pitakpaivan et al., 1994; Bohor and Glass, 1995; Smit et al., 1996; Schulte et al., 2006; Witts et al., 2018).

4.2. Evidence for depositional processes from macrofaunal analysis

Macrofaunal analysis of units I and II indicates a core group of abundant molluscan taxa that occur in all horizons: *Breviarca* (*Striarca) webbervillensis*, *Malletia longifrons, N. travisana*, *Cymbophora cancellosa*, and *Vetericardiella webbervillensis*. We propose that these abundant taxa were derived locally, implying that in both Unit I and Unit II, there was substantial input from the same or an environment proximal to the underlying Corsicana Formation. These taxa were also found to be common components of the Cretaceous macrofaunal community in previous faunal evaluations at the Brazos River localities (Hansen et al. 1987; Hansen et al., 1993a; Hansen et al., 1993b).

Outside of the core taxa, most other faunal elements are found only within a single sampled horizon, with little overlap (overlap is defined here as a species occurring in two or more samples). In the four sampled horizons, two representing the Corsicana Formation and one each representing Unit I and Unit II, there are three groups of taxa that are unique to each unit. We suggest that these unique taxa are indicative of sediment transport from different environmental settings in both units I and II, and that these three units were formed by distinct depositional processes that derived sediment and bioclasts from different sources.

Taphonomic analysis shows that the same mode of molluscan preservation, mostly complete single valves, is dominant in each unit. However, Unit I contains a higher percentage of articulated bivalves relative to the underlying Corsicana Formation, and Unit II has the highest percentage of articulated bivalves. We interpret this to mean that the conditions of fossilization in the Corsicana Formation were slow, allowing time for organisms to decay and disaggregate, resulting in a lower number of articulated specimens. Conversely, conditions of fossilization in unit I and II were rapid, allowing burial of some articulated specimens.

Mode of life analysis also shows minimal differences between the Corsicana Formation, Unit I, and Unit II. The same categories of mobility, feeding, and tiering dominate in all units except for a

broader spread of mobile and immobile taxa in the Corsicana Formation. However, mode of life does differ within the rarer elements of each faunal assemblage. The occurrence of two feeding strategies in units I and II which do not occur in the underlying Corsicana Formation can be interpreted as increased incorporation of allochthonous bioclasts. It is also possible that these occurrences are due to an increase in time averaging due to the higher density of bioclasts in Unit I and Unit II compared to the underlying Corsicana. Unit I has similar sedimentological characteristics as the underlying Corsicana Formation. Based on the sedimentology, it is most probable that an increase in time averaging (e.g. higher density of bioclasts) accounts for the greater diversity of modes of life within Unit I. Conversely, Unit II has very different sedimentological characteristics and has a higher relative abundance of modes of life which either do not appear or are rare in the underlying Corsicana Formation. The explanation that these are allochthonous bioclasts is therefore considered most viable.

There is an increase in fauna with a non-motile, attached, cemented lifestyle in Unit II (the bivalve genera *Anomia* and *Ostrea*). It is not clear if this signal is local (e.g., derived from the underlying Corsicana Formation) or a result of the input of allochthonous elements. Encrusting organisms require hard surfaces to adhere onto, which would be more abundantly available in an environment closer to shore. However, *Eubaculites* shells encrusted with oysters are commonly found in the Corsicana Formation (Hansen et al., 1987; Witts et al., 2021). These ‘benthic islands’ are common immediately below or within a few centimeters of the K-Pg boundary and are therefore not reflected in our Corsicana samples, taken at 0.5m and 1.25 m below the K-Pg.

The increase in carnivores/predators in Unit II compared to other units can be interpreted as the incorporation of allochthonous faunal elements during deposition. The taxa in Unit II that belong to the carnivore/predatory feeding strategy have two genera in common with the Corsicana Formation but also include three genera and five species not present in the underlying units. These unique taxa are considered allochthonous elements and reflect transport of foreign shells into this area from another, distinctly different, habitat.

A compilation of benthic mollusk data throughout the latest Cretaceous of the USA Gulf Coastal Plain shows that carnivores/predators were much rarer in offshore environments compared to shallow, nearshore environments, that host more abundant populations of taxa with these modes of life (Sessa et al. 2012). We therefore interpret these allochthonous faunal elements in Unit II as sourced from a more proximal or shallower water environment where carnivore/predator fauna were more abundant.

4.3. Evidence for depositional processes from sedimentology

Unit I — The mode of deposition of Unit I is interpreted as a cohesive debris flow (Gani, 2004; Mulder and Alexander, 2001). Soft sediment deformation and sediment injection into the underlying Corsicana Formation further suggest rapid deposition on a seismically disturbed sea floor. Other prominent sedimentary features are a chaotic fabric, muddy matrix, lack of grading, and transport of boulders and pebble-sized material (Fig. 2). The largest boulder at DMC measures 20 cm across the long axis, indicating transport in a flow with considerable matrix strength. Chaotic fabric and lack of grading (grain size analysis restricted to fine fraction of sediment) reflects deposition by freezing of the flow (Mulder and Alexander 2001; Gani, 2004; Talling et al., 2012). These depositional constraints are best explained by a high strength cohesive debris flow. The mobilization of sediment could be attributed to ground shaking, liquefaction, and partial shelf collapse, resulting from the Chicxulub bolide impact (Bralower et al., 2010; Denne et al., 2013; Sanford et al. 2016; Renne et al., 2018; Gulick et al., 2019). This debris flow would have been highly localized. Grain size data shows that the matrix has the same mean grain size (fine silt) as the Corsicana Formation, with both showing a similar grain size distribution (Fig. 6) suggesting the debris flow mobilized local sediment, primarily from similar environments to the Corsicana Formation.

Yancey and Liu (2013) interpret Unit I to be a stratified gravity-driven dense flow, with only the basal most “denser debris flow” preserved. The high concentration of bioclasts excludes, for Yancey and Liu (2013), the interpretation that it is a cohesive flow of any kind. They argue that if the flow were cohesive, it would more closely resemble the Corsicana Formation, a bioclast poor mud – siltstone. Non-cohesive debris flow deposits are identified based on the lack of cohesive material within the flow,

amongst other features (Talling et al., 2012). This is not observed in the deposits of Unit I we have studied. Grain size analysis shows that the matrix of this deposit is mud rich (>62.5 μm). Therefore, we favor the interpretation that Unit I was deposited by a cohesive debris flow. The concentration of bioclasts can be explained by ground shaking and turbulence, which disturbed Corsicana Formation shales and began suspending clay and silt into the water column prior to sediment mobilization. Disturbed Corsicana Formation at Cottonmouth Creek, which we consider locally analogous to Unit I, contains concentrations of bioclasts but apparently was not disturbed enough to create a sediment flow.

The presence of carbonate lapilli but apparent lack of a significant number of impact spherules in Unit I is interesting. If this were a diagenetic feature, one might expect to see features such as microcrystalline calcite representing relict spherule material, but this was not recorded in our extensive examination of Unit I. Assuming these units were deposited rapidly post-impact, it could indicate a primary depositional feature and reflect differential arrival times of lapilli vs. spherules at this location ~1500 km from the impact site. However, studies that have evaluated carbonate lapilli related to Chicxulub and other impact events suggest these features formed in the main vapor plume alongside the glassy impact spherules (Pope et al., 2005; Yancey and Guillemette, 2008; Salge et al., 2021). Uncertainties remain about the precise mode of ejecta transport and deposition following impact (see Artemieva and Morgan (2020) for a recent discussion). A possible factor for the stratification of these ejecta, if they arrived at the same time, are variable settling velocities of the clasts through the shallow water column, but further study is required.

Unit II — The mode of deposition for Unit II was probably a cohesive debris flow. Features consistent with deposition via cohesive debris flow are abrupt pinching out on topographic highs, allochthonous shell material, high mud content in the matrix and inverse grading (Talling et al., 2012). A muddy, and therefore cohesive, matrix would have the strength to travel considerable distance across the shelf, bringing allochthonous faunal elements from adjacent environments (Simm et al., 1991; Kidwell and Bosence, 1991). A muddy, cohesive, matrix would also have enough strength to entrain larger clasts, such as sand sized grains and bioclasts, which are common in this deposit (Fig. 6). Unit II, in contrast to

Unit I, does not contains cobble or boulder sized clasts. The lack of outsized clasts suggests this unit was formed by a low – medium strength cohesive debris flow (Talling et al., 2012). Although inverse grading is not common in debris flow deposits, it can occur when the uppermost surface interacts with turbulence in the water column (Talling et al., 2012).

The increase in the clay sized fraction up-section is interpreted as being partially due to post-depositional alteration of originally glassy impact spherules to smectite (see Pitakpaivan et al. (1994)). Chemical analysis performed by Keller et al. (2007) of the "spherule – rich coarse sandstone unit (SCS)", equivalent to Unit II, indicates that smectite percentages are near 100%. The bimodal curve may have been skewed towards a coarser grain size fraction before diagenesis of spherules, that varied in size but were up to ~2mm in diameter. Unit II is interpreted as inversely graded, despite an increase in the clay sized sediment fraction up section based on the presence of diagenetically altered spherules.

Unit II is interpreted as a debrite. What triggered deposition is not entirely clear. However, fossils more common in nearshore settings found within this deposit indicate sediment transport from more proximal environments. Compositional and sedimentological features of this deposit differ greatly from Unit I, despite a similar interpretation for mode of deposition. This implies that seismic energy alone cannot explain this deposit, an additional or separate factor was required to move these sediments. We suggest two explanations. A passing tsunami wave could have created this flow deposit as backwash incorporating shallower water elements, transporting them across the shelf. Equivalent sections in the Brazos area (Brazos-1) have been shown to contain elevated soil organic matter in Unit II (Vellekoop et al., 2014; Vellekoop et al., 2018), also consistent with the interpretation of this unit as a tsunami backwash deposit. Similar units interpreted as tsunami backwash deposits are found in the La Popa Basin, Mexico (Schulte et al., 2012; Le Roux and Vargas, 2005). Recent study by Kinsland et al. (2021) reveal the scale of sedimentary features left by the tsunami in Gulf of Mexico shelf settings following the Chicxulub impact; seismic data revealed the presence of 'mega ripples' preserved at the K-Pg boundary in the subsurface. With wavelengths of ~600 m and heights of up to 16 m these features formed in water depths similar to those proposed for Brazos, below storm wave base.

This unit could also be the result of partial shelf collapse in the region; sediment gravity flow deposits coinciding with the K-Pg boundary in the deep-water Gulf of Mexico have been linked to this process post-impact (Denne et al., 2013; Sanford et al.; 2016). Alternatively, as noted above, Unit II could have formed as result of a combination of both these processes, with seismogenic failure of the shelf either triggering tsunami formation, or material disturbed by earthquakes and liquefaction being rapidly redistributed across the shelf by the passage of tsunami wave trains. Similar processes have been suggested recently to explain formation of K-Pg deposits in the eastern Gulf of Mexico (Poag, 2017) and along the Pacific margin in Baja California, Mexico (Santa Catharina et al., 2022).

Yancey and Liu (2013) interpreted Unit II as a lag deposit, based on the lack of transport indicators and heterogenous composition. We argue that the presence of allochthonous fauna, and inverse grading make it improbable that this unit is the result of local wave oscillation currents. Movement of shells from shoreward environments to deeper water is not common during storms events and therefore it is unlikely that a deposit containing allochthonous elements is the result of storm wave oscillation currents (Kreisa, 1981; Warme et al., 1976). It is much more common to find allochthonous elements in sediment flow (turbidite, debrite) and slump deposits (Kidwell and Bosence, 1991). Lag deposits are typically capped by silt/mud deposits that record the fallout of suspended fine-grained sediment during the waning of storm wave energy; Unit II does not preserve a mud/silt cap. It is possible that a finer settling out layer was deposited and subsequently eroded. However, Unit II coarsens upward and shows no sign of recording deposition via waning current energy. There is also evidence for injection of Unit II into disturbed upper Corsicana Formation shales (which we consider analogous to Unit I) along CMC (Figure 4), further suggesting rapid deposition. Based on these features it is most likely that Unit II is the result of a sediment flow and not storm wave oscillation currents.

Lateral variations in thickness of Unit I and Unit II across the Brazos outcrop belt (e.g., Hansen et al., 1987; Smit et al., 1996; Schulte et al., 2006) is indicative of localized and channelized deposition. Channels may have existed as paleo-seafloor topography, as has been suggested by Yancey (1996) and Yancey and Liu (2013) who noted that the relief and variability in thickness exhibited by the K-Pg

boundary complex at Brazos suggests local scouring of the seafloor of up to 2 m. If these channels represent topographic features on the Cretaceous seafloor as suggested by Hart et al. (2012) and Yancey and Liu (2013), it is likely they were further excavated by high energy deposition of the boundary complex – apparent in the incorporation of material from the Corsicana Formation in Unit I.

4.4. Timing of deposition and links to the Chicxulub impact

Several models now exist which calculate the timing of post-impact events in detail (Pope et al., 2005; Collins et al., 2005; Sanford et al., 2016; Gulick et al., 2019; Salge et al., 2021). Though each model prescribes slightly different timing, the order of events is generally consistent for sites proximal to the Chicxulub crater:

1) arrival of seismic waves

2) ejecta fallout

3) tsunami wave passage

4) settling of dust and fine ejecta

We recognize that some of these events were at times coeval and note that the given order is specifically for time of first arrival at any given location. In addition, the potential stratigraphic record of these events is likely complicated by ongoing disruption following impact; for example, repeated tsunami or seiche events in the Gulf of Mexico triggered by platform or crater collapse events occurring years-decades after impact (e.g., Gulick et al., 2019; Whalen et al., 2020).

The timing of deposition of Unit I is apparently constrained by lack of abundant impact spherules, yet possible association with seismic energy. Models predict that seismic energy from a magnitude 10-11 ‘mega-quake’ arrived within minutes to proximal localities along the Gulf Coastal Plain, with ejecta arriving within minutes to hours (Sanford et al., 2016; Witts et al., 2018; Gulick et al., 2019; Santa Catharina et al., 2022). Based on this we suggest that the deposition of Unit I occurred within minutes to hours of the Chicxulub impact.

The exact timing of deposition of Unit II is difficult to determine because it is not clear if seismic energy, shelf collapse or tsunami wave energy mobilized these sediments. Unit II contains an appreciable

amount of impact ejecta in the form of spherules and carbonate lapilli; however, their concentration suggests that ejecta were mobilized from elsewhere on the shelf and concentrated in this deposit. While we agree that this unit does contain evidence for 'reworking' (Hart et al., 2012), the timescale over which this reworking occurred could therefore have been remarkably short. Although it appears unlikely based on the current analyses and previous work (see discussion in Hart et al., 2019), further work is needed to determine if either of these units contain any evidence of true air-fall deposition, and whether the apparent difference in concentration between carbonate lapilli and spherules is at all a reliable marker for timing and nature of depositional processes.

If we accept the interpretation that Unit II is a tsunami backwash deposit, the timing can be better constrained using modeled tsunami landfall timing. Tsunamis would have begun arriving at GCP localities within hours of impact, but wave energy would have mostly dissipated within days (Range et al., 2022). However, repeated local tsunami events may have continued to affect proximal GCP localities during the earliest decades/centuries of the Danian. Unit II would have been deposited within this window (Sanford et al., 2016).

The uppermost unit identified in the Brazos K-Pg deposits, the silt/clay upward fining fourth unit or 'CCH', contains proxy evidence for a ~6°C decline in sea surface temperatures (Vellekoop et al., 2014), and an iridium anomaly (Ganapathy et al., 1981; Asaro et al., 1982; Hildebrand et al., 1992; Hansen et al., 1993b; Rocchia et al., 1996; results compiled in Vellekoop et al., 2014). An 'impact winter' related to global darkness and massive formation of atmospheric sulfate aerosols likely lasted decades after impact (Brugger et al., 2017; Junium et al., 2022). The iridium anomaly is not found in the underlying units and provides an additional upward limit on timing for Unit I, Unit II, and the HCS sandstone units. Recent estimates of settling times for iridium suspended in the dust cloud initiated by the Chicxulub impact, suggest fallout took~20 years at minimum (Goderis et al., 2021). The scattered and 'smeared out' nature of the Ir profile in the Brazos deposits suggests some reworking and resuspension by turbulence in the water column as a result of post-impact perturbations, which could extend the settling time to a century (Vellekoop et al., 2014) or at most, thousands of years (Goderis et al., 2013; Schulte et

al., 2010). Using these conservative estimates, the timing of deposition for the lower portion of the K-Pg event deposits at Brazos is on the scale of minutes to decades (<20 years) or conservatively centuries, with the entire event deposit formed within decades to at most, thousands of years.

4.5. Relation to upper units of the K-Pg boundary complex

Above Unit II, the rest of the K-Pg boundary complex at DMC is made up of interbedded hummocky cross stratified (HCS) sandstones and siltstones. At DMC-W, the lower HCS sandstone contains impact spherules. The interpretation of this part of the K-Pg boundary complex is that it either records tsunami deposition (Bourgeois et al., 1988; Smit et al., 1996) or a series of storm deposits formed after the impact event during the earliest Danian (Yancey and Liu, 2013). Siltstone layers interbedded between the HCS sandstone units contain microfossils (foraminifera and nannofossils) (Hart et al., 2019), and thin (2-5 cm-thick) layers rich in macrofossils – primarily bivalves (oysters), and scaphopods. It has been suggested that these represent quiescent periods with recolonization of the sea floor and are incompatible with tsunami or other very rapid deposition.

We examined the thick siltstone interval intercalated between the HCS sandstone units at the DMC outcrop in 2019 (Fig. 2). This revealed that the siltstone unit also contains obvious hummocky cross-stratification throughout, with several (2-3) thin shell-rich layers, and shelly material generally draped along the lee slopes of the hummocks. Although not obvious in the DMC outcrop, the presence of burrows in this and other intervals in the upper part of the event deposit has also been used to argue for prolonged deposition. However, in a recent re-study of the K-Pg boundary units at Moscow Landing in Alabama, Savrda (2018) argued that burrows in these shallow marine impact deposits can form very quickly and do not necessarily indicate lengthy deposition. Similarly, Rodríguez-Tovar et al. (2020) describe burrowing activity in sediments within the Chicxulub crater itself within years of impact – even prior to final atmospheric fallout of impact debris (Goderis et al., 2021). Such a scenario is consistent with the Ir profile from Brazos (Vellekoop et al., 2014). We suggest that a detailed re-study of the ichnology of the upper portion of the K-Pg event deposit at Brazos (both HCS and CCH units – which does not outcrop at the DMC-W site we studied) is required with these new data in mind.

4.6. Implications for sea level fall hypothesis at the K-Pg boundary

The hypothesis that this unit represents an early transgressive system tract deposit or is the result of sea level fall (Keller et al., 2007; Gale, 2006) is not supported by the data collected herein. Soft sediment deformation structures (sediment injected into disturbed Corsicana Formation mudstones) indicate that Unit I and Unit II were deposited rapidly during a time of seismic disturbance. This does not align with the interpretation of these deposits happening after large storms. Because of the apparent stratification of different kinds of impact ejecta between the units I (carbonate lapilli) and unit II (carbonate lapilli and spherules), it is improbable that all impact ejecta is remobilized from lower in the Corsicana Formation (Keller et al. 2007).

Previous interpretations of orange clay-rich layers in the Corsicana Formation below the K-Pg event deposit as 'altered spherule layers' (e.g., Keller et al., 2007; Keller and Adatte, 2011) have been invalidated by detailed study, which confirms their origin as volcanic ash layers (Hart et al., 2012; Hart et al., 2019). Additionally, depth approximation based on foraminiferal and microfossil data suggest similar water depths of 50-150 m during both the latest Maastrichtian and early Paleogene in the Brazos River area (Yancey and Liu, 2013; Woelders and Speijer, 2015). Suggestions for paleosol development in the Brazos River area based on the occurrence of plant rootlets and gypsum crystals in the Mullinax-3 drill core (Adatte et al., 2011) have also been challenged by Yancey and Liu (2013) and Hart et al. (2012; 2019), who argue instead that these represent Pleistocene river terrace deposits unrelated to K-Pg processes.

These observations align with evidence from the eastern Gulf Coastal Plain that water depth did not drop below the shelf break during the K-Pg interval (Hart et al., 2013), before a sea level fall in the Danian (Savrda et al., 2018; Witts et al., 2018). Additionally, although macrofauna in Unit I and Unit II suggest mixing of material from different environments, the fauna lacks any profound signal of water depth changes expected during a shallowing event. The modes of life of fauna largely remains the same, and therefore we suggest any allochthonous input is the result of transport from an adjacent environment on the shelf – not representing an establishment of a shallow water community.

5. Conclusions

Detailed examination of the basal units of the K-Pg event deposit along the Brazos River, Texas show features consistent with mass movement of sediment during the immediate aftermath of the Chicxulub impact at a site proximal to the crater. Faunal analysis and sedimentological features indicate flows with different characteristics at the time of deposition are responsible for formation of these units:

1) Unit I contains mainly locally-derived fauna and sedimentary material and was deposited by a high strength cohesive debris flow, as a conglomeratic debrite. This process was most likely initiated by intense ground shaking generated by earthquakes following the Chicxulub impact event.
2) Unit II contains impact spherules, allochthonous bioclasts from nearshore settings and has different sedimentological features than either Unit I or the underlying Corsicana Formation. This unit was deposited by a medium-low strength cohesive debris flow. This process was most likely initiated by tsunami wave energy, as a result of shelf collapse, or some combination of these two processes over a short timescale.

Our data add to a growing body of evidence that sediment flows, driven by the release of seismic energy and combined with the action of large tsunami waves, were a major factor in transport of large amounts of sedimentary material following the Chicxulub impact in the Gulf of Mexico, even in relatively shallow (<100 m) settings (Soria et al., 2002; Schulte et al. 2012; Denne et al., 2013; Sanford et al., 2016; Witts et al., 2018). Further study of these deposits, ongoing work on the Chicxulub crater itself (e.g., Whalen et al., 2020) and study of other K-Pg deposits in shallow settings in the Gulf of Mexico combined with subsurface imaging on a regional scale (e.g., Kinsland et al., 2021) will help elucidate the aftermath of this important event in Earth history and its proximal environmental effects in unprecedented detail.

Acknowledgements

We are hugely grateful to Mr. and Mrs. Ronnie and Jackie Mullinax (Brazos Rose Ranch) for allowing access to their property for fieldwork, and their generous hospitality. We thank Tom Yancey, Carlie

Pietsch, Ekaterina Larina, Remy Rovelli, Paul Renne, Isabel Fendley, Linda Ivany, Chris Junium, Ben Uveges, and Shibajyoti Das for useful discussions and assistance in the field. At the AMNH, we thank Mariah Slovacek for assistance with specimen preparation and SEM analysis, and Steve Thurston for assistance with figures. At Brooklyn College we thank Shannon Brophy, Jone Naujokaityte for useful discussions, and Natalie Dastas for her mentorship and access to petrographic microscopes. At Penn State we thank Claire Cleveland and Heather Jones for their feedback on preliminary figures and interpretations. This research was funded by the Louis Stokes Alliance for Minority Participation and the National Science Foundation, the Rosen Fellowship at Brooklyn College, and a Lerner-Gray Postdoctoral Research Fellowship at the American Museum of Natural History and Richard Gilder Graduate School awarded to James Witts. Additional funding was provided by the Norman Newell Fund (AMNH).

References

Aberhan, M., Kiessling, W., 2015. Persistent ecological shifts in marine molluscan assemblages across the end-Cretaceous mass extinction. PNAS 112, 7207–7212. https://doi.org/10.1073/pnas.1422248112

Abramovich, S., Keller, G., Berner, Z., Cymbalista, M., Rak, C., 2011. Maastrichtian Planktic Foraminiferal Biostratigraphy and Paleoenvironment of Brazos River, Falls County, Texas, U.S.A., in: Keller, G., Adatte, T. (Eds.), The End-Cretaceous Mass Extinction and the Chicxulub Impact in Texas. SEPM Society for Sedimentary Geology, Tulsa, pp. 43–80. https://doi.org/10.2110/sepmsp.100.123

Adatte, T., Keller, G., Baum, G.R., 2011. Age and Origin of the Chicxulub Impact and Sandstone Complex, Brazos River, Texas: Evidence from Lithostratigraphy and Sedimentology, in: Keller, G., Adatte, T. (Eds.), The End-Cretaceous Mass Extinction and the Chicxulub Impact in Texas. SEPM Society for Sedimentary Geology, Tulsa, pp. 43–80. https://doi.org/10.2110/sepmsp.100.043

Akers, R., Akers, T., 2002a. Texas Cretaceous bivalves 2, Texas paleontology series. Paleontological Section, Houston Gem and Mineral Society, Houston.

Akers, R., Akers, T., 2002b. Texas Cretaceous gastropods, Texas paleontology series. Paleontological Section, Houston Gem and Mineral Society, Houston.

Alvarez, L.W., Alvarez, W., Asaro, F., Michel, H.V., 1980. Extraterrestrial Cause for the Cretaceous-Tertiary Extinction. Science 208, 1095–1108. http://doi.org/10.1126/science.208.4448.1095

Alvarez, W., 2019. A review of the Earth history record in the Cretaceous, Paleogene, and Neogene pelagic carbonates of the Umbria-Marche Apennines (Italy): twenty-five years of the Geological Observatory of Coldigioco. In 250 million years of Earth history in Central Italy: celebrating 25 years of the Geological Observatory of Coldigioco. Geological Society of America Special Paper, 1-58. https://doi.org/10.1130/2019.2542(01)

Artemieva, N., Morgan, J. 2020. Global K-Pg layer deposited from a dust cloud. Geophysical Research Letters 47, e2019GL086562. https://doi.org/10.1029/2019GL086562

Asaro, F., Alvarez, L.W., Alvarez, W., Michel, H.V., 1982. Geochemical anomalies near the Eocene/Oligocene and Permian/Triassic boundaries, in: Silver, L.T., Schultz, P.H. (Eds.), Geological Implications of Impacts of Large Asteroids and Comets on the Earth. Geological Society of America, Boulder, pp. 517–528. https://doi.org/10.1130/SPE190-p517

Bambach, R.K., 2006. Phanerozoic Biodiversity Mass Extinctions. Annual Review of Earth and Planetary Sciences 34, 127.

Bell, H.S., 1940. Armored Mud Balls: Their Origin, Properties, and Role in Sedimentation. The Journal of Geology 48, 1–31. http://doi.org/10.1086/624859

Bohor, B.F., 1996. A sediment gravity flow hypothesis for 27iliclastic units at the K/T boundary, northeastern Mexico, in: Ryder, G., Fastovsky, D., and Gartner, S. (Eds.), The Cretaceous – Tertiary Event and Other Catastrophes in Earth History: Geological Society of America, Special Paper 307, Boulder, pp. 183-196. https://doi.org/10.1130/0-8137-2307-8.183

Bohor, B.F., Glass, B.P., 1995. Origin and diagenesis of K/T impact spherules: from Haiti to Wyoming and beyond. Meteoritics 30, 182- 198.

Bourgeois, J., Hansen, T.A., Wiberg, P.L., Kauffman, E.G., 1988. A Tsunami Deposit at the Cretaceous-Tertiary Boundary in Texas. Science 241, 567–570. https://doi.org/10.1126/science.241.4865.567

Bralower, T., Eccles, L., Kutz, J., Yancey, T., Schueth, J., Arthur, M., Bice, D., 2010. Grain size of Cretaceous – Paleogene boundary sediments from Chicxulub to the open ocean: Implications for interpretation of the mass extinction event. Geology 38, 199–202. https://doi.org/10.1130/G30513.1

Brugger, J., Feulner, G., Petri, S., 2017. Baby, it's cold outside: Climate model simulations of the effects of the asteroid impact at the end of the Cretaceous. Geophysical Research Letters 44, 419–427. https://doi.org/10.1002/2016GL072241@10.1002/(ISSN)1944-8007.2016GRLEDHIGH

Burtt, D.G., Henkes, G.A., Yancey, T.E., Schrag, D., 2022. Hot atmospheric formation of carbonate accretionary lapilli at the Cretaceous-Paleogene boundary, Brazos River, Texas, from clumped isotope thermometry. Geology 50, 636–640. https://doi.org/10.1130/G49674.1

698 Cita, M.B., Aloisi, G., 2000. Deep-sea tsunami deposits triggered by the explosion of Santorini (3500y
699 BP), eastern Mediterranean. Sedimentary Geology 135, 181–203. https://doi.org/10.1016/S0037-
700 0738(00)00071-3
701
702 Collins, G.S., Melosh, H.J., Marcus, R.A., 2005. Earth Impact Effects Program: A Web-based computer
703 program for calculating the regional environmental consequences of a meteoroid impact on Earth.
704 Meteoritics & Planetary Science 40, 817–840. https://doi.org/10.1111/j.1945-5100.2005.tb00157.x
705
706 Conrad, T.A., 1853. Synopsis of the Family of Naides of North America; with notes and a table of some
707 of the genera and subgenera. Journal of the Natural Sciences of Philadelphia 8, 183–190.
708
709 Conrad, T.A., 1857. Descriptions of Cretaceous and Tertiary Fossils. Report of the United States and
710 Mexican Boundary Survey 1, 141–174.
711
712 Conrad, T.A., 1858. Observations on a Group of Cretaceous Fossil Shells, Found in Tippah County,
713 Mississippi, with Descriptions of Fifty-six New Species. Journal of the Academy of Natural Science of
714 Philadelphia 3, 323–336.
715
716 Conrad, T.A., 1860. Description of New Species of Cretaceous and Eocene Fossils of Mississippi and
717 Alabama. Journal of the Academy of Natural Sciences of Philadelphia 4, 275–298.
718
719 Denne, R.A., Scott, E.D., Eickhoff, D.P., Kaiser, J.S., Hill, R.J., Spaw, J.M., 2013. Massive Cretaceous-
720 Paleogene boundary deposit, deep-water Gulf of Mexico: New evidence for widespread Chicxulub-
721 induced slope failure. Geology 41, 983–986. https://doi.org/10.1130/G34503.1
722

DePalma, R.A., Smit, J., Burnham, D.A., Kuiper, K., Manning, P.L., Oleinik, A., Larson, P., Maurrasse, F.J., Vellekoop, J., Richards, M.A., Gurche, L., Alvarez, W., 2019. A seismically induced onshore surge deposit at the KPg boundary, North Dakota. PNAS 116, 8190–8199. https://doi.org/10.1073/pnas.1817407116

During, M.A.D., Smit, J., Voeten, D.F.A.E., Berruyer, C., Tafforeau, P., Sanchez, S., Stein, K.H.W., Verdegaal-Warmerdam, S.J.A., van der Lubbe, J.H.J.L., 2022. The Mesozoic terminated in boreal spring. Nature 603, 91–94. https://doi.org/10.1038/s41586-022-04446-1

Fujiwara, O., 2008. Bedforms and Sedimentary Structures Characterizing Tsunami Deposits, in: Shiki, T., Tsuji, Y., Yamazaki, T., Minoura, K. (Eds.), Tsunamiites. Elsevier, Amsterdam, pp. 51–62. https://doi.org/10.1016/B978-0-444-51552-0.00004-7

Gabb, W.M., 1860. Descriptions of New Species of American Tertiary and Cretaceous Fossils. Journal of the Academy of Natural Sciences of Philadelphia 4, 375–406.

Gale, A.S., 2006. The Cretaceous—Palaeogene boundary on the Brazos River, Falls County, Texas: is there evidence for impact-induced tsunami sedimentation? Proceedings of the Geologists' Association 117, 173–185. https://doi.org/10.1016/S0016-7878(06)80008-8

Galloway, W.E., Ganey-Curry, P.E., Li, X., Buffler, R.T., 2000. Cenozoic Depositional History of the Gulf of Mexico Basin. AAPG Bulletin 84, 1743–1774. https://doi.org/10.1306/8626C37F-173B-11D7-8645000102C1865D

Ganapathy, R., Gartner, S., Jiang, M.-J., 1981. Iridium anomaly at the Cretaceous-Tertiary boundary in Texas. Earth and Planetary Science Letters 54, 393–396. https://doi.org/10.1016/0012-821X(81)90055-8

Gani, M.R., 2004. From turbid to lucid: a straightforward approach to sediment gravity flows and their deposits. The Sedimentary Record, 2, 4-8. http://doi.org/10.2110/sedred.2004.3.4

Gardner, J.A., 1916. Systematic Paleontology, Mollusca. Maryland Geological Survey Upper Cretaceous, 371–733.

Goderis, S., Tagle, R., Belza, J., Smit, J., Montanari, A., Vanhaecke, F., Erzinger, J., Claeys, Ph., 2013. Reevaluation of siderophile element abundances and ratios across the Cretaceous–Paleogene (K–Pg) boundary: Implications for the nature of the projectile. Geochimica et Cosmochimica Acta 120, 417–446. https://doi.org/10.1016/j.gca.2013.06.010

Goderis, S., Sato, H., Ferrière, L., Schmitz, B., Burney, D., Kaskes, P., Vellekoop, J., Wittmann, A., Schulz, T., Chernonozhkin, S.M., Claeys, P., de Graaff, S.J., Déhais, T., de Winter, N.J., Elfman, M., Feignon, J.-G., Ishikawa, A., Koeberl, C., Kristiansson, P., Neal, C.R., Owens, J.D., Schmieder, M., Sinnesael, M., Vanhaecke, F., Van Malderen, S.J.M., Bralower, T.J., Gulick, S.P.S., Kring, D.A., Lowery, C.M., Morgan, J.V., Smit, J., Whalen, M.T., IODP-ICDP EXPEDITION 364 SCIENTISTS, 2021. Globally distributed iridium layer preserved within the Chicxulub impact structure. Science Advances 7, eabe3647. https://doi.org/10.1126/sciadv.abe3647

Gulick, S.P.S., Bralower, T.J., Ormö, J., Hall, B., Grice, K., Schaefer, B., Lyons, S., Freeman, K.H., Morgan, J.V., Artemieva, N., Kaskes, P., de Graaff, S.J., Whalen, M.T., Collins, G.S., Tikoo, S.M., Verhagen, C., Christeson, G.L., Claeys, P., Coolen, M.J.L., Goderis, S., Goto, K., Grieve, R.A.F., McCall, N., Osinski, G.R., Rae, A.S.P., Riller, U., Smit, J., Vajda, V., Wittmann, A., 2019. The first day of the Cenozoic. PNAS 116, 19342–19351. https://doi.org/10.1073/pnas.1909479116

775 Hansen, T., Farrand, R.B., Montgomery, H.A., Billman, H.G., Blechschmidt, G., 1987. Sedimentology
776 and extinction patterns across the Cretaceous-Tertiary boundary interval in east Texas. Cretaceous
777 Research 8, 229–252. https://doi.org/10.1016/0195-6671(87)90023-1
778
779 Hansen, T.A., Farrell, B.R., Upshaw, B., 1993a. The first 2 million years after the Cretaceous-Tertiary
780 boundary in east Texas: rate and paleoecology of the molluscan recovery. Paleobiology 19, 251–265.
781 https://doi.org/10.1017/S0094837300015906
782
783 Hansen, T.A., Upshaw, B., Kauffman, E.G., Gose, W., 1993b. Patterns of molluscan extinction and
784 recovery across the Cretaceous-Tertiary boundary in east Texas; report on new outcrops. Cretaceous
785 Research 14, 685–706. https://doi.org/10.1006/cres.1993.1047
786
787 Hart, M.B., Leighton, A.D., Hampton, M., Smart, C.W., 2019. Global bioevents and the
788 Cretaceous/Paleogene boundary in Texas and Alabama: Stratigraphy, correlation and ocean acidification.
789 Global and Planetary Change 175, 129–143. https://doi.org/10.1016/j.gloplacha.2019.01.020
790
791 Hart, M.B., Yancey, T.E., Leighton, A.D., Miller, B., Liu, C., Smart, C.W., Twitchett, R.J., 2012. The
792 Cretaceous-Paleogene Boundary on the Brazos River, Texas: New Stratigraphic Sections and Revised
793 Interpretations. Gulf Coast Association of Geological Societies Journal 1, 69–80.
794
795 Henehan, M.J., Ridgwell, A., Thomas, E., Zhang, S., Alegret, L., Schmidt, D.N., Rae, J.W.B., Witts, J.D.,
796 Landman, N.H., Greene, S.E., Huber, B.T., Super, J.R., Planavsky, N.J., Hull, P.M., 2019. Rapid ocean
797 acidification and protracted Earth system recovery followed the end-Cretaceous Chicxulub impact. PNAS
798 116, 22500–22504. https://doi.org/10.1073/pnas.1905989116
799

Hildebrand, A.R., 1992. Geochemistry and stratigraphy of the Cretaceous/Tertiary boundary impact ejecta. (Ph.D. Dissertation). The University of Arizona.

Hill, R.T., 1893. Paleontology of the Cretaceous Formations of Texas: The Invertebrate Paleontology of the Trinity Division. Proceedings of the Biological Society of Washington 8, 97–108.

Hull, P.M., Bornemann, A., Penman, D.E., Henehan, M.J., Norris, R.D., Wilson, P.A., Blum, P., Alegret, L., Batenburg, S.J., Bown, P.R., Bralower, T.J., Cournede, C., Deutsch, A., Donner, B., Friedrich, O., Jehle, S., Kim, H., Kroon, D., Lippert, P.C., Loroch, D., Moebius, I., Moriya, K., Peppe, D.J., Ravizza, G.E., Röhl, U., Schueth, J.D., Sepúlveda, J., Sexton, P.F., Sibert, E.C., Śliwińska, K.K., Summons, R.E., Thomas, E., Westerhold, T., Whiteside, J.H., Yamaguchi, T., Zachos, J.C., 2020. On impact and volcanism across the Cretaceous-Paleogene boundary. Science 367, 266–272. https://doi.org/10.1126/science.aay5055

Jiang, M.J., Gartner, S., 1986. Calcareous nannofossil succession across the Cretaceous/Tertiary boundary in east-central Texas. Micropaleontology 32, 232–255.

Junium, C.K., Zerkle, A.L., Witts, J.D., Ivany, L.C., Yancey, T.E., Liu, C., Clare, M.W., 2022. Massive perturbations to atmospheric sulfur in the aftermath of the Chicxulub impact. PNAS 119, e2119194119. https://doi.org/10.1073/pnas.2119194119

Keller, G., Adatte, T., Berner, Z., Harting, M., Baum, G., Prauss, M., Tantawy, A., Stueben, D., 2007. Chicxulub impact predates K–T boundary: New evidence from Brazos, Texas. Earth and Planetary Science Letters 255, 339–356. https://doi.org/10.1016/j.epsl.2006.12.026

Kennedy, W.J., Gale, A.S., Hansen, T.A., 2001. The last Maastrichtian ammonites from the Brazos River sections in Falls County, Texas. Cretaceous Research 22, 163–171. https://doi.org/10.1006/cres.2001.0245

Kidwell, S., Bosence, D.W., 1991. Taphonomy and time-averaging of marine shelly faunas., in: Taphonomy: Releasing the Data Locked in the Fossil Record. Plenum, New York, pp. 115–209.

Kinsland, G.L., Egedahl, K., Strong, M.A., Ivy, R., 2021. Chicxulub impact tsunami megaripples in the subsurface of Louisiana: Imaged in petroleum industry seismic data. Earth and Planetary Science Letters 570, 117063. https://doi.org/10.1016/j.epsl.2021.117063

Kreisa, R.D., 1981. Storm-generated sedimentary structures in subtidal marine facies with examples from the Middle and Upper Ordovician of southwestern Virginia. Journal of Sedimentary Research 51, 823–848. https://doi.org/10.1306/212F7DBF-2B24-11D7-8648000102C1865D

Kring, D.T., Petruny, L.W., 2008. Impact spherule-bearing Cretaceous–Tertiary sand body, Shell Creek stratigraphic section, Alabama, USA, in: Evans, K.R., Horton, D.T., King, Jr., Morrow, J.R. (Eds.), The Sedimentary Record of Meteorite Impacts, Geological Society of America Special Paper 437. Boulder, pp. 179–187.

Le Roux, J.P., Vargas, G., 2005. Hydraulic behavior of tsunami backflows: insights from their modern and ancient deposits. Environmental Geology 49, 65–75. https://doi.org/10.1007/s00254-005-0059-2

Leighton, A.D., Hart, M.B., Smart, C.W., Leng, M.J., Hampton, M., 2017. Timing Recovery After the Cretaceous/paleogene Boundary: Evidence from the Brazos River, Texas, Usa. Journal of Foraminiferal Research 47, 229–238. https://doi.org/10.2113/gsjfr.47.3.229

Lyons, S.L., Karp, A.T., Bralower, T.J., Grice, K., Schaefer, B., Gulick, S.P.S., Morgan, J.V., Freeman, K.H., 2020. Organic matter from the Chicxulub crater exacerbated the K–Pg impact winter. PNAS 117, 25327–25334. https://doi.org/10.1073/pnas.2004596117

Maechler, M., Rousseeuw, P., Struyf, A., Hubert, M., Hornik, K., 2018. cluster: Cluster Analysis Basics and Extensions. R package version 2.0.7.

McCune, B., Grace, J.B. and Urban, D.L., 2002. Analysis of ecological communities. MJM software design, Gleneden Beach.

Molina, E., Alegret, L., Arenillas, I., Arz, J.A., Gallala, N., Hardenbol, J., Salis, K.V., Steurbaut, E., Vandenberghe, N. and Zaghbib-Turki, D., 2006. The global boundary stratotype section and point for the base of the Danian stage (Paleocene, Paleogene," Tertiary", Cenozoic) at El Kef, Tunisia-original definition and revision. Episodes 29, 263–273. https://doi.org/10.18814/epiiugs/2006/v29i4/004

Morton, S.G., 1833. Supplement to the “Synopsis of the Organic Remains of the Ferruginous Sand Formation of the United States.” American Journal of Science 23, 288–297.

Morton, S.G., 1834. Synopsis of the Organic Remains of the Cretaceous Group of the United States. Key and Biddle, Philadelphia.

Mulder, T., Alexander, J., 2001. The physical character of subaqueous sedimentary density flows and their deposits. Sedimentology 48, 269–299. https://doi.org/10.1046/j.1365-3091.2001.00360.x

Oksanen, J., Blanchet, G.F., Friendly, M., Kindt, R., Legendre, P., McGlinn, D., Minchin, P.R., O'Hara, R.B., Simpson, G.L., Solymos, P., Stevens, M.H.H., Szoecs, E., Wagner, H., 2019. vegan: Community Ecology Package, R package version 2.5-5.

Olszewski, T.D., 2015. Abrupt global shifts in ecosystem states. PNAS 112, 7111–7112. https://doi.org/10.1073/pnas.1507590112

Plummer, H.J., 1927. Foraminifera of the Midway Formation in Texas. University of Texas Bulletin 2644, 1–206.

Pitakpaivan, K., Byerly, G.R., Hazel, J.E. 1994. Pseudomorphs of impact spherules from a Cretaceous-Tertiary boundary section at Shell Creek, Alabama. Earth and Planetary Science Letters 124, 49-56. https://doi.org/10.1016/0012-821X(94)00077-8

Poag, C.W., 2017. Shaken and stirred: Seismic evidence of Chicxulub impact effects on the West Florida carbonate platform, Gulf of Mexico. Geology 45, 1011–1014. https://doi.org/10.1130/G39438.1

Pope, K.O., Ocampo, A.C., Fischer, A.G., Vega, F.J., King, D.T.Jr., Fouke, B.W., Wachtman, R.J., Kletetschka, G., 2005. Chicxulub impact ejecta deposits in southern Quintana Roo, México, and central Belize, in: Kenkmann T, Horz F, Deustch A (Eds.), Large Meteorite Impacts III, Large Meteorite Impacts. Geological Society of America Special Papers 384, Boulder, pp. 171-190. https://doi.org/10.1130/0-8137-2384-1.171

R Core Team., 2017. R: A language and environment for statistical computing. R Foundation for Statistical Computing, Vienna, Austria. Available at: http://www.R-project.org/

Range, M.M., Arbic, B.K., Johnson, B.C., Moore, T.C., Titov, V., Adcroft, A.J., Ansong, J.K., Hollis, C.J., Ritsema, J., Scotese, C.R., Wang, H., 2022. The Chicxulub Impact Produced a Powerful Global Tsunami. AGU Advances 3, e2021AV000627. https://doi.org/10.1029/2021AV000627

Raup, D.M., Sepkoski, J.J., 1982. Mass Extinctions in the Marine Fossil Record. Science 215, 1501–1503. https://doi.org/10.1126/science.215.4539.1501

Renne, P.R., Arenillas, I., Arz, J.A., Vajda, V., Gilabert, V., Bermúdez, H.D., 2018. Multi-proxy record of the Chicxulub impact at the Cretaceous-Paleogene boundary from Gorgonilla Island, Colombia. Geology 46, 547–550. https://doi.org/10.1130/G40224.1

Rocchia, R., Robin, E., Froget, L., Gayraud, J., 1996. Stratigraphic distribution of extraterrestrial markers at the Cretaceous-Tertiary boundary in the Gulf of Mexico area: Implications for the temporal complexity of the event, in: Ryder, G., Fastovsky, D.E., Gartner, S. (Eds.), The Cretaceous-Tertiary Event and Other Catastrophes in Earth History. Geological Society of America, Boulder, pp. 279–286. https://doi.org/10.1130/0-8137-2307-8.279

Rodríguez-Tovar, F.J., Lowery, C.M., Bralower, T.J., Gulick, S.P.S., Jones, H.L., 2020. Rapid macrobenthic diversification and stabilization after the end-Cretaceous mass extinction event. Geology 48, 1048–1052. https://doi.org/10.1130/G47589.1

Salge, T., Tagle, R., Schmitt, R-T., Hecht, L. 2021. Petrographic and chemical studies of the Cretaceous-Paleogene boundary sequence at El Guayal, Tabasco, Mexico: implications for ejecta plume evolution

from the Chicxulub impact crater. In Reimold, W.U., and Koeberl, C. (Eds.), Large Meteorite Impacts and Planetary Evolution VI: Geological Society of America Special Paper 550, Boulder, pp. 207-233.

Sanford, J.C., Snedden, J.W., Gulick, S.P.S., 2016. The Cretaceous-Paleogene boundary deposit in the Gulf of Mexico: Large-scale oceanic basin response to the Chicxulub impact. Journal of Geophysical Research: Solid Earth 121, 1240–1261. https://doi.org/10.1002/2015JB012615

Santa Catharina, A., Kneller, B.C., Marques, J.C., McArthur, A.D., Cevallos-Ferriz, S.R.S., Theurer, T., Kane, I.A., and Muirhead, D.A. 2022. Timing and causes of forest fire at the K–Pg boundary. Scientific Reports 12, 13006. https://doi.org/10.1038/s41598-022-17292-y

Savrda, C.E., 2018. Revisiting the origins of Clayton sand bodies at the K-Pg transition, Moscow Landing, Western Alabama: stratigraphic relations, sedimentology, and ichnology. PALAIOS 33, 555–567. https://doi.org/10.2110/palo.2018.086

Schulte, P., Alegret, L., Arenillas, I., Arz, J.A., Barton, P.J., Bown, P.R., Bralower, T.J., Christeson, G.L., Claeys, P., Cockell, C.S., Collins, G.S., Deutsch, A., Goldin, T.J., Goto, K., Grajales-Nishimura, J.M., Grieve, R.A.F., Gulick, S.P.S., Johnson, K.R., Kiessling, W., Koeberl, C., Kring, D.A., MacLeod, K.G., Matsui, T., Melosh, J., Montanari, A., Morgan, J.V., Neal, C.R., Nichols, D.J., Norris, R.D., Pierazzo, E., Ravizza, G., Rebolledo-Vieyra, M., Reimold, W.U., Robin, E., Salge, T., Speijer, R.P., Sweet, A.R., Urrutia-Fucugauchi, J., Vajda, V., Whalen, M.T., Willumsen, P.S., 2010. The Chicxulub Asteroid Impact and Mass Extinction at the Cretaceous-Paleogene Boundary. Science 327, 1214–1218. https://doi.org/10.1126/science.1177265

Schulte, P., Smit, J., Deutsch, A., Salge, T., Friese, A., Beichel, K., 2012. Tsunami backwash deposits with Chicxulub impact ejecta and dinosaur remains from the Cretaceous–Palaeogene boundary in the La Popa Basin, Mexico. Sedimentology 59, 737–765. https://doi.org/10.1111/j.1365-3091.2011.01274.x

Schulte, P., Speijer, R., Mai, H., Kontny, A., 2006. The Cretaceous–Paleogene (K–P) boundary at Brazos, Texas: Sequence stratigraphy, depositional events and the Chicxulub impact. Sedimentary Geology 184, 77–109. https://doi.org/10.1016/j.sedgeo.2005.09.021

Sessa, J.A., Bralower, T.J., Patzkowsky, M.E., Handley, J.C., Ivany, L.C., 2012. Environmental and biological controls on the diversity and ecology of Late Cretaceous through early Paleogene marine ecosystems in the U.S. Gulf Coastal Plain. Paleobiology 38, 218–239. https://doi.org/10.1666/10042.1

Sheehan, P.M., Hansen, T.A., 1986. Detritus feeding as a buffer to extinction at the end of the Cretaceous. Geology 14, 868–870. https://doi.org/10.1130/0091-7613(1986)14<868:DFAABT>2.0.CO;2

Shumard, B.F., 1861. Descriptions of New Cretaceous Fossils from Texas. Proceedings of the Boston Society of Natural History 8, 188–205.

Simm, R.W., Weaver, P.P.E., Kidd, R.B., Jones, E.J.W., 1991. Late Quaternary mass movement on the lower continental rise and abyssal plain off Western Sahara. Sedimentology 38, 27–40. https://doi.org/10.1111/j.1365-3091.1991.tb01853.x

Smit, J., Reop, T.B., Alvarez, W., Montanari, A., Claeys, P., Grajales- Nishimura, J.M., Bermudez, J., 1996. Coarse-grained, clastic sandstone complex at the KT boundary around the Gulf of Mexico: deposition by tsunami waves induced by the Chicxulub impact?, in: Ryder, G., Fastovsky, D.,

Gartner, S. (Eds.), The Cretaceous–Tertiary Event and Other Catastrophes in Earth History: Geological Society of America, Special Paper 307, Boulder, pp. 151–182. https://doi.org/10.1130/0-8137-2307-8.151

Sohl, N., 1960. Archeogastropoda, Mesogastropoda, and stratigraphy of the Ripley, Owl Creek, and Prairie Bluff formations. Geological Survey Professional Paper 331, 1–151.

Soria, A.R., Liesa, C.L., Mata, M.P., Arz, J.A., Alegret, L., Arenillas, I., Meléndez, A., 2001. Slumping and a sandbar deposit at the Cretaceous-Tertiary boundary in the El Tecolote section (northeastern Mexico): An impact-induced sediment gravity flow. Geology 29, 231–234. https://doi.org/10.1130/0091-7613(2001)029<0231:SAASDA>2.0.CO;2

Stephenson, L.W., 1917. North American Upper Cretaceous corals of the genus Micrabacia. USGS Numbered Series, Professional Paper 98, 115–131. https://doi.org/10.3133/pp98J

Stephenson, L.W., 1941. The Larger Invertebrate Fossils of the Navarro Group. The University of Texas Publication, Austin.

Stephenson, L.W., 1955. Owl Creek (Upper Cretaceous) fossils from Crowleys Ridge, southeastern Missouri. United States Geological Survey Professional Paper 274, 97–140.

Talling, P.J., Masson, D.G., Sumner, E.J., Malgesini, G., 2012. Subaqueous sediment density flows: Depositional processes and deposit types. Sedimentology 59, 1937–2003. https://doi.org/10.1111/j.1365-3091.2012.01353.x

Vaughan, T.W., 1900. The Eocene and lower Oligocene coral faunas of the United States, with descriptions of a few doubtfully Cretaceous species. USGS Numbered Series, Monograph 263. https://doi.org/10.3133/m39

Vellekoop, J., Esmeray-Senlet, S., Miller, K.G., Browning, J.V., Sluijs, A., van de Schootbrugge, B., Sinninghe Damsté, J.S., Brinkhuis, H., 2016. Evidence for Cretaceous-Paleogene boundary bolide "impact winter" conditions from New Jersey, USA. Geology 44, 619–622. https://doi.org/10.1130/G37961.1

Vellekoop, J., Sluijs, A., Smit, J., Schouten, S., Weijers, J.W.H., Sinninghe Damsté, J.S., Brinkhuis, H., 2014. Rapid short-term cooling following the Chicxulub impact at the Cretaceous–Paleogene boundary. PNAS 111, 7537–7541. https://doi.org/10.1073/pnas.1319253111

Vellekoop, J., Woelders, L., van Helmond, N.A.G.M., Galeotti, S., Smit, J., Slomp, C.P., Brinkhuis, H., Claeys, P., Speijer, R.P., 2018. Shelf hypoxia in response to global warming after the Cretaceous-Paleogene boundary impact. Geology 46, 683–686. https://doi.org/10.1130/G45000.1

Warme, J.E., Ekdale, A.A., Ekdale, S.F., Peterson, C.H., Scott, R.W. and West, R.R., 1976. Raw material of the fossil record. In: Scott R.W., West R.W. (Eds.), Structure and classification of paleocommunities. Dowden, Hutchinson and Ross, Stroudsburg, pp. 143-169.

Weller, S., 1907. A Report on the Cretaceous Fauna of New Jersey. Geological Survey of New Jersey, Paleontology 4.

Wentworth, C.K., 1922. A Scale of Grade and Class Terms for Clastic Sediments. The Journal of Geology 30, 377–392. https://doi.org/10.1086/622910

Whalen, M.T., Gulick, S.P.S., Lowery, C.M., Bralower, T.J., Morgan, J.V., Grice, K., Schaefer, B., Smit, J., Ormö, J., Wittmann, A., Kring, D.A., Lyons, S., Goderis, S., 2020. Winding down the Chicxulub impact: The transition between impact and normal marine sedimentation near ground zero. Marine Geology 430, 106368. https://doi.org/10.1016/j.margeo.2020.106368

Witts, J.D., Landman, N.H., Garb, M.P., Boas, C., Larina, E., Rovelli, R., Edwards, L.E., Sherrell, R.M., Cochran, J.K., 2018. A fossiliferous spherule-rich bed at the Cretaceous–Paleogene (K–Pg) boundary in Mississippi, USA: Implications for the K–Pg mass extinction event in the Mississippi Embayment and Eastern Gulf Coastal Plain. Cretaceous Research 91, 147–167. https://doi.org/10.1016/j.cretres.2018.06.002

Witts, J.D., Landman, N.H., Garb, M.P., Irizarry, K.M., Larina, E., Thibault, N., Razmjooei, M.J., Yancey, T.E. and Myers, C.E., 2021. Cephalopods from the Cretaceous-Paleogene (K-Pg) boundary interval on the Brazos River, Texas, and extinction of the ammonites. American Museum Novitates, 2020, 1-52. https://doi.org/10.1206/3964.1

Woelders, L., Speijer, R. 2015. Stable seafloor conditions, sea level and food supply during the latest Maastrichtian at Brazos River, Texas. Marine Micropaleonotology 121, 41-51.

Yancey, T.E., 1996. Stratigraphy and Depositional Environments of the Cretaceous-Tertiary Boundary Complex and Basal Paleocene section, Brazos River, Texas. Gulf Coast Association of Geological Transactions 46, 433-442.

Yancey, T.E., Guillemette, R.N., 2008. Carbonate accretionary lapilli in distal deposits of the Chicxulub impact event. GSA Bulletin 120, 1105–1118. https://doi.org/10.1130/B26146.1

Yancey, T.E., Liu, C., 2013. Impact-Induced Sediment Deposition On An Offshore, Mud-Substrate Continental Shelf, Cretaceous–Paleogene Boundary, Brazos River, Texas, U.S.A Brazos Cretaceous–Paleogene Boundary. Journal of Sedimentary Research 83, 354–367. https://doi.org/10.2110/jsr.2013.30

Figures and captions

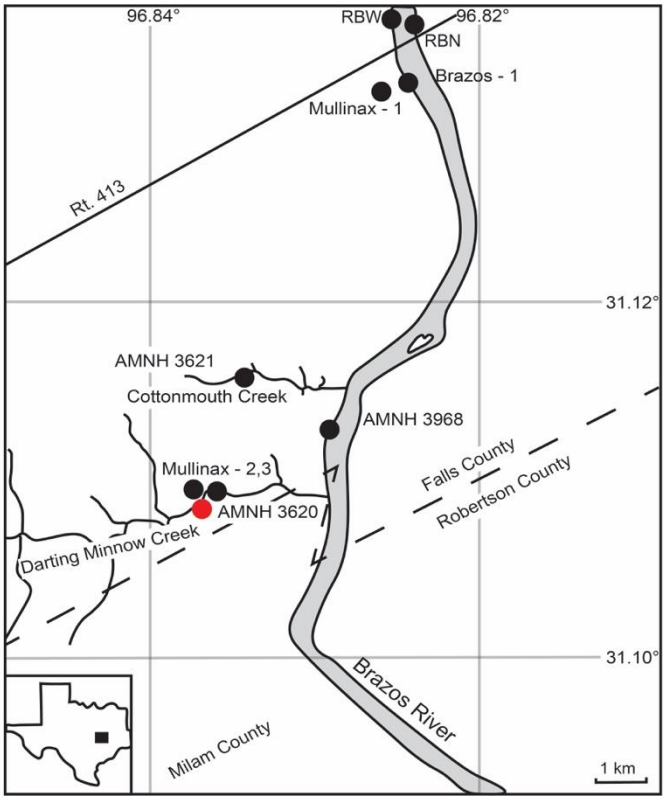

Figure. 1 Map of Brazos River, Texas, with localities and cores mentioned in the text shown as circles. Red circle indicates the waterfall section in Darting Minnow Creek (AMNH locality 3620, DMC-W), the main sampling locality. Abbreviated sites are River Bed West (RBW) and River Bed North (RBN).

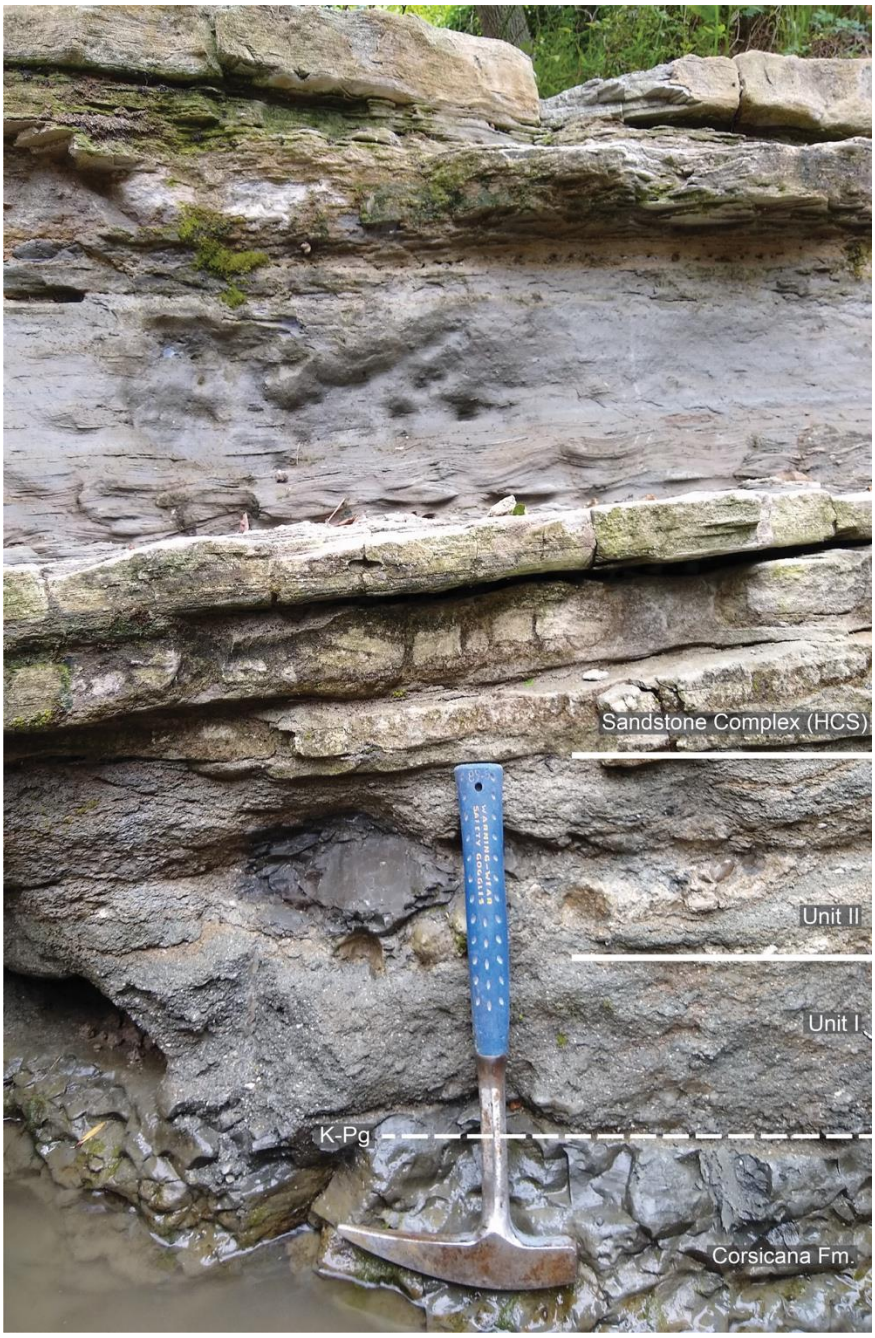

Figure. 2 Outcrop photo taken at the Darting Minnow Creek waterfall section (DMC-W) (AMNH Locality 3620) showing the Corsicana Formation, the basal mudstone-clast-bearing unit (Unit I), the

ejecta-spherule-rich coarse sandstone (Unit II) and the sandstone complex (HCS). Exact location where photo was taken is highlighted by the white rectangle in the overview photo of DMC-W (Fig. 3).

Figure. 3 A zoomed out view of Darting Minnow Creek waterfall section (DMC-W) (AMNH Locality 3620) taken in 2019 showing the Corsicana Formation and the K-Pg event deposit, which becomes more expanded towards the right. Large, rafted clasts and ovoid micritic concretions are visible at the contact between unit I and II. The white rectangle highlights the area where a close-up image of the event complex was taken (Fig. 2). Note that the placement of the K-Pg boundary (dashed white line) differs from that illustrated in Hart et al. (2012) and Hart et al. (2019) (compare to Figure 5 in Hart et al. (2019)).

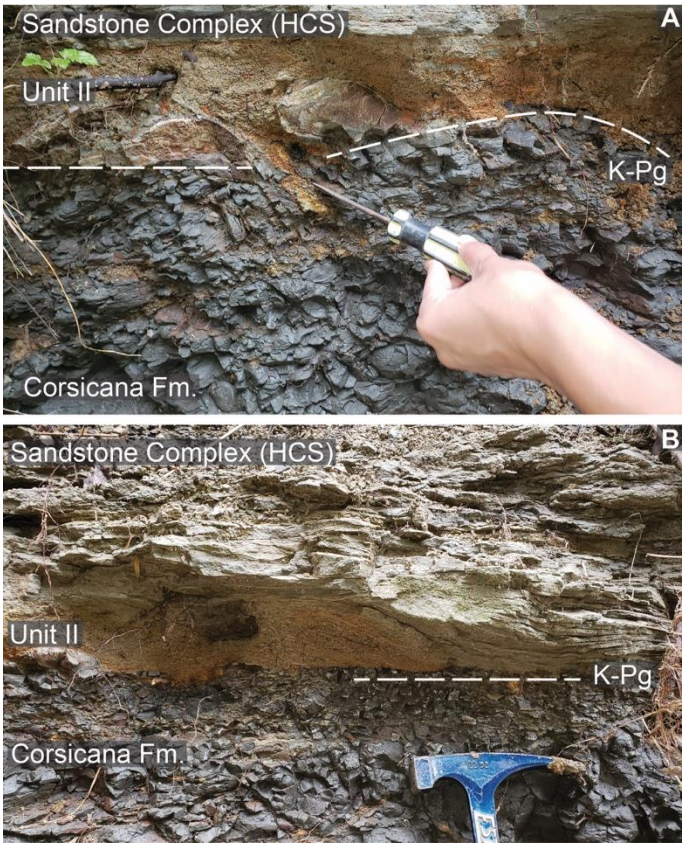

Figure 4. Photos taken along the lower part of Cotton Mouth Creek (CMC) (AMNH Locality 3621) of the disturbed Corsicana Formation Shale and the K-Pg event complex. A) Unit II directly overlies disturbed Corsicana Formation shales; variable sheets of micritic cement visible at contact; screwdriver indicates injection of Unit II into disturbed shales; small section of Sandstone complex visible at top of photo. B) Unit II pinches out towards the right over a short distance until the sandstone unit directly overlies disturbed Corsicana Formation shales.

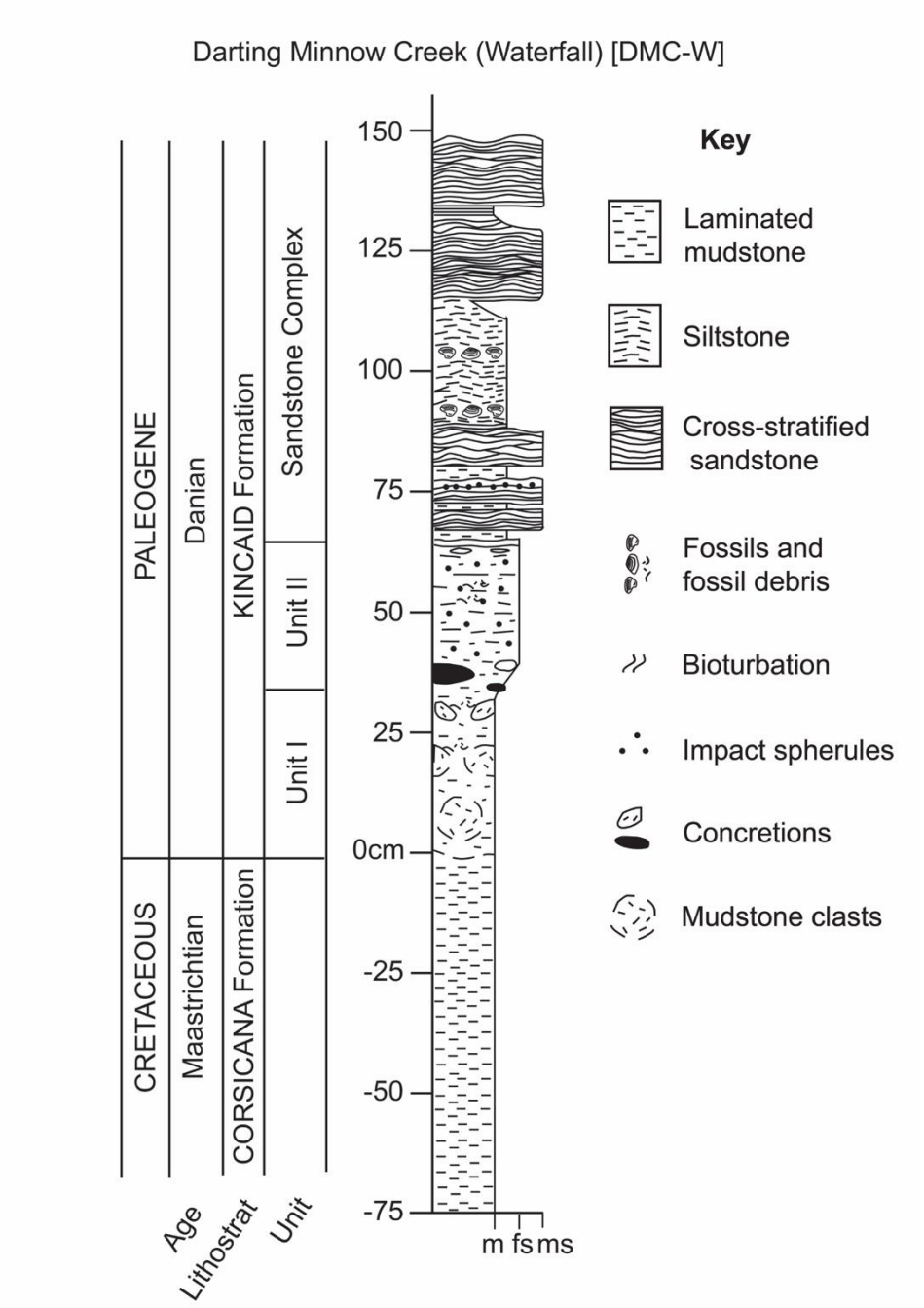

1108

1109

1110 **Figure 5.** Stratigraphic column and sedimentary log of of K-Pg complex at Darting Minnow Creek

1111 Waterfall (DMC-W) (AMNH locality 3620). Note that concretions in the section are pre-existing and

1112 derived.

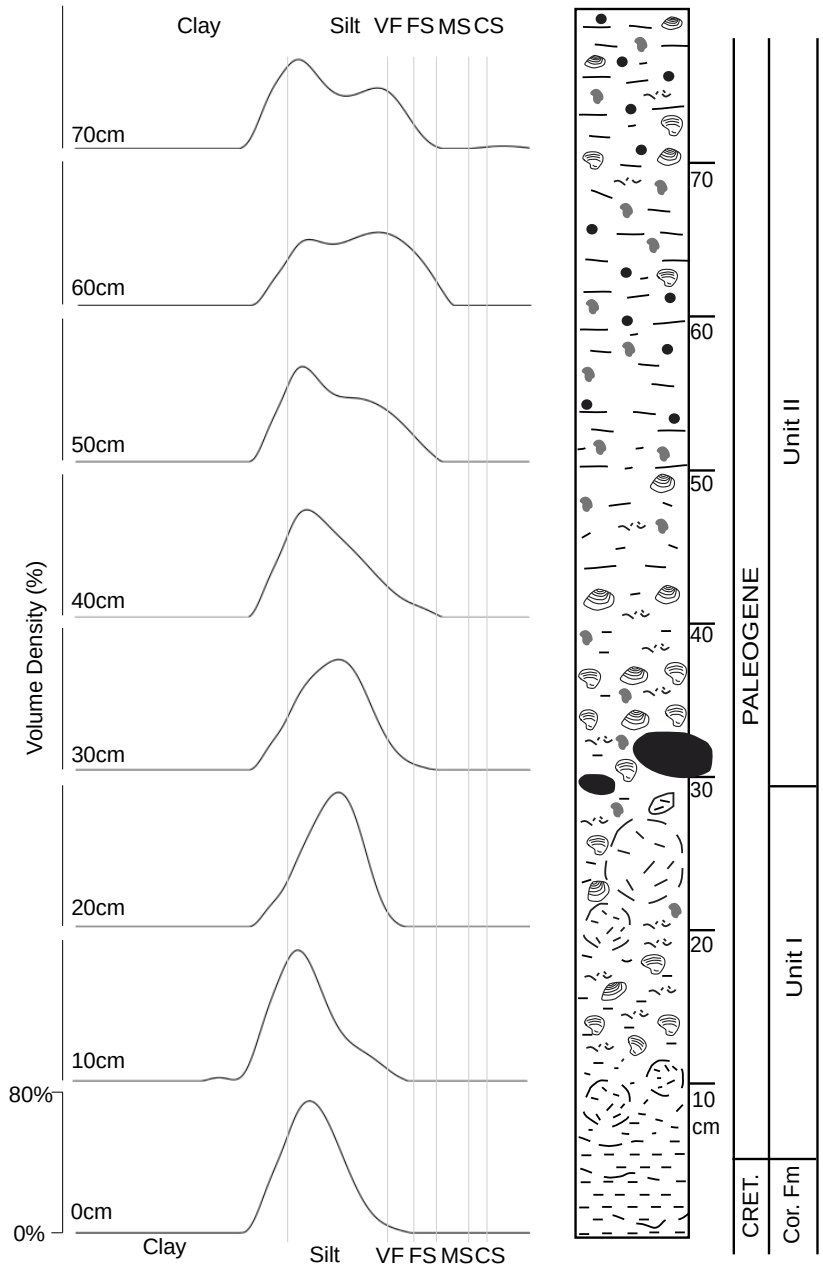

Figure 6. Grain size distribution curves (%), analysis using a Malvern Mastersizer 3000; all calcium carbonate and organic matter were removed from samples. The x-axis is a logged grain size scale, with grains binned according to the Wentworth grain size classification chart (Wentworth, 1922). Samples

were taken at 10 cm intervals starting at the base of the core (Corsicana Formation) and through the basal most K-Pg boundary complex (units I and II) at the DMC-W outcrop. Diagrammed core log (Sup. Fig. 1) to the right of distribution curves, legend for symbols can be found in Figure 5.

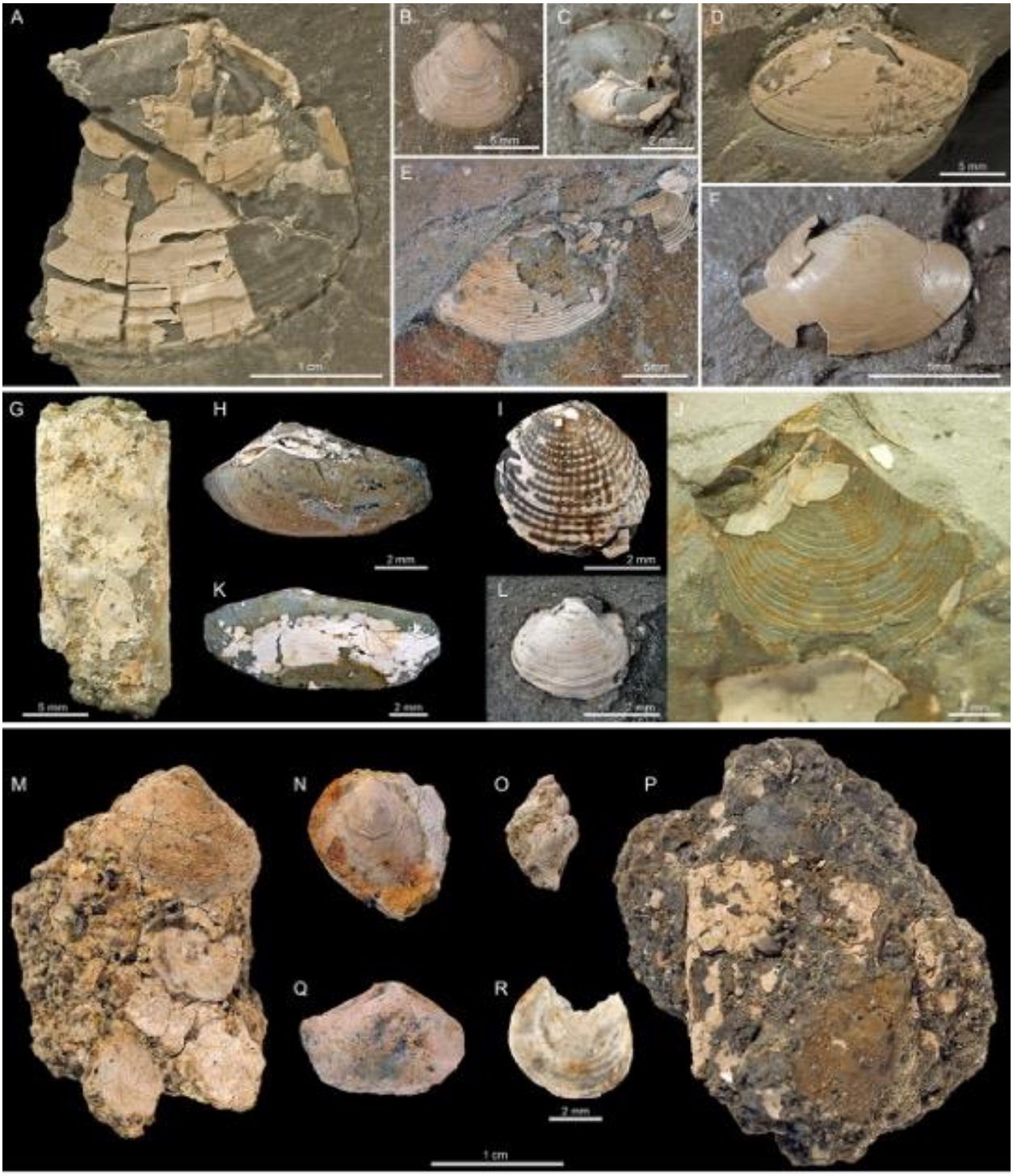

1124

1125 **Figure 7.** Representative fauna from each unit. Corsicana Fm A – F, Unit I G – J, Unit II M – P; A –

1126 *Cyprimeria depressa* Conrad, 1860, B – *Syncyclonema archeri* Stephenson, 1941 , C – *Breviarca*

(*Striarca) webbervillensis* Stephenson, 1941, D – *Nuculana Corsicana* Stephenson, 1941, E – *Cymbophora cancellosa* Stephenson, 1941, F – *Nuculana coloradoensis* Stephenson, 1941, G – *Eubaculites carinatus* Morton, 1834, H – *Nuculana travisana* Stephenson, 1941, I – *Vetercardiella webbervillensis* Stephenson, 1941, J – *Syncyclonema simplicus* Conrad, 1860, Indet. nuculanid. K – *Malletia longifrons* Conrad, 1860, L – *Breviarca* (*Striarca) webbervillensis* Stephenson, 1941, M – *Cymbophora cancellosa* Stephenson, 1941, N – *Camptonectes bubonis* Stephenson, 1941, O – *Paladmete alta* Stephenson, 1941, P – *Eubaculites* sp., Q – *Nuculana travisana* Stephenson, 1941, R – *Anomia texana*. Hill, 1893

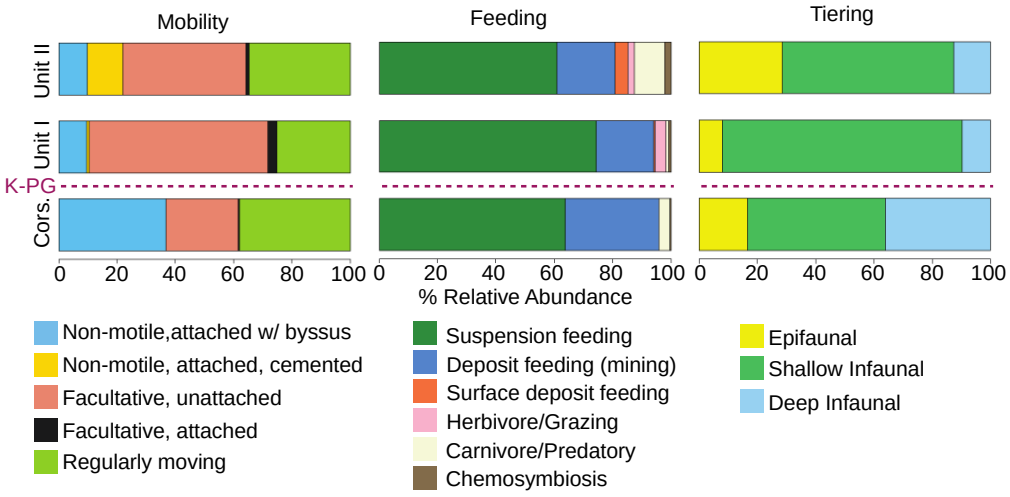

Figure 8. Mode of life broken down according to mobility, feeding and tiering, as determined by Aberhan and Kiessling (2015) supplementary document. Relative abundance is plotted on the x-axis (%), with units ordered in stratigraphic order on the y-axis. The Corsicana Formation has been amalgamated into one representative unit for this analysis.

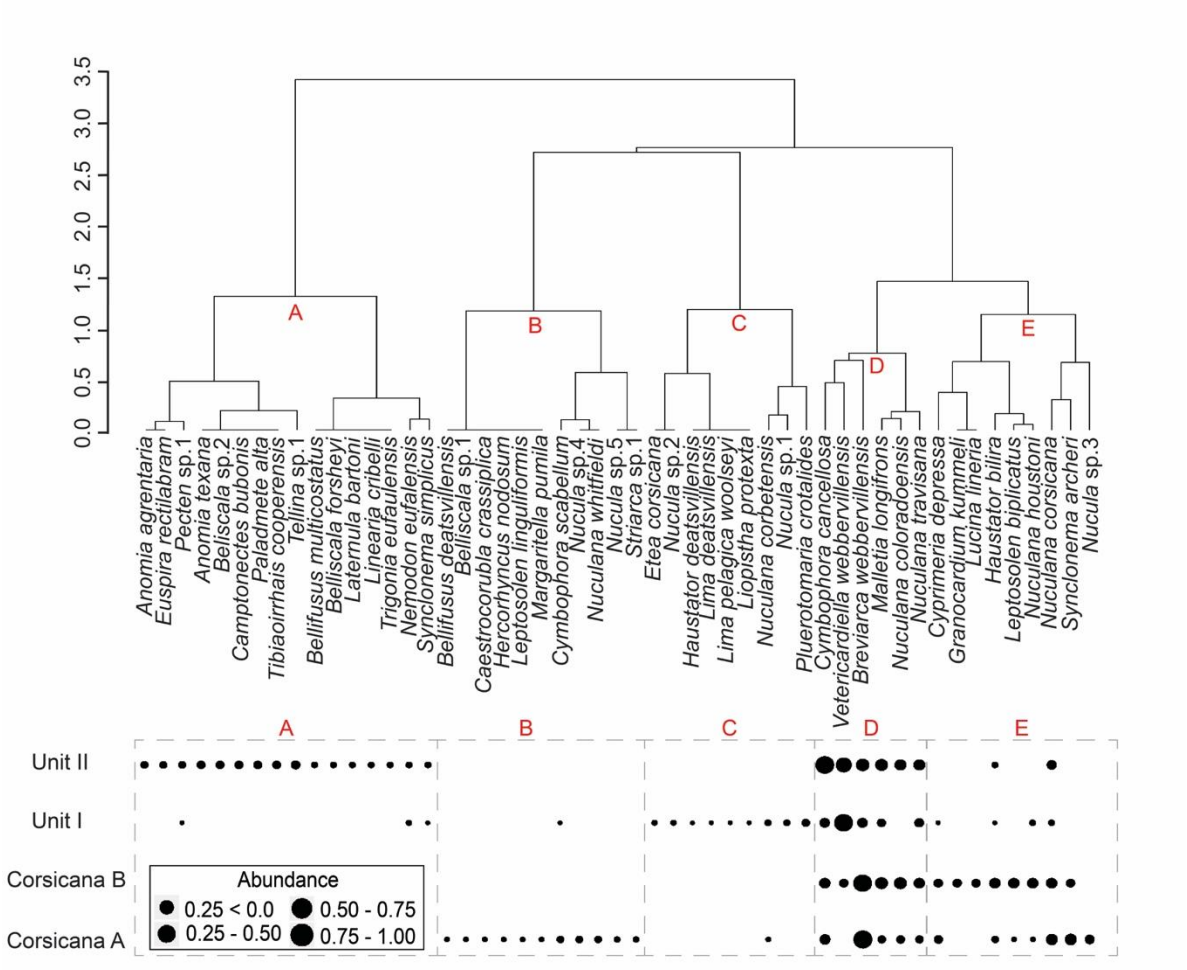

Figure 9. Species level cluster analysis performed using Bray – Curtis distance measure, and Ward's linkage method made in R v.3.3.3 (R Core Team, 2017). Dot plot corresponds to units on stratigraphic column (Fig. 5). Corsicana A sampled at 1.25m below the K-Pg boundary, Corsicana B sampled 0.5m below the K-Pg boundary. Dots scaled to abundance counts.